NASA Contractor Report 182123

Measurement of Unsteady Blade Surface Pressure on a Single Rotation Large Scale Advanced Prop-Fan With Angular and Wake Inflow at Mach Numbers From 0.02 to 0.70

P. Bushnell, M. Gruber, and D. Parzych

Hamilton Standard
Windsor Locks, Connecticut

October 1988

Prepared for
Lewis Research Center
Under Contract NAS3-23051

Date for general release October 1990

National Aeronautics and
Space Administration

CONTENTS

SUMMARY

Unsteady aerodynamic pressures were measured on the surface of a rotating Prop-Fan blade in an experiment performed by Hamilton Standard Division of United Technologies Corporation, under contract to NASA-Lewis Research Center, at the S1-MA wind tunnel facility operated by the office National D'Etudes et de Recherches Aerospatiale (ONERA) in Modane, France.

The objectives of the experiment were to measure the periodic variations of blade surface pressure resulting from two non-uniform inflow conditions: first, inflow at a three degree angle to the Prop-Fan axis of rotation, and second, inflow with a wake generated by a cylinder mounted upstream of the rotor.

In addition, unsteady pressures were measured under uniform inflow conditions to determine background response levels. The range of Prop-Fan operating conditions included inflow Mach numbers from 0.02 to 0.70. For most of the inflow Mach numbers, more than one power coefficient and/or advance ratio was investigated.

Due to facility power limitations the Prop-Fan test installation was a two bladed version of the eight bladed design configuration. The power coefficient range investigated was therefore selected to cover typical power loading per blade conditions which occur within the Prop-Fan operating envelope.

This report provides unsteady blade surface pressure data for the LAP Prop-Fan blade operation with angular inflow, wake inflow and uniform flow over a range of inflow Mach numbers of 0.02 to 0.70. The data are presented as Fourier coefficients for the first 35 harmonics of shaft rotational frequency. Also presented is a brief discussion of the unsteady blade response observed at takeoff and cruise conditions with angular and wake inflow.

INTRODUCTION

Prop-Fans are high cruise speed, single or counter rotation, highly loaded, variable pitch advanced turboprops designed to operate at high cruise speeds. Prop-Fan blades incorporate thin airfoils with sweep and are integrated with a spinner and nacelle shaped to reduce axial Mach number through the rotor. This configuration minimizes compressibility losses and results in higher propulsive efficiency than is achievable by high bypass ratio turbofans.

Since 1974 NASA-sponsored Prop-Fan research at Hamilton Standard has proceeded through a series of wind tunnel studies of model Prop-Fans, to the current Large Scale Advanced Prop-Fan (LAP) program and then to the follow-on Prop-Fan Test Assessment (PTA) flight test program.

Over the last several years it has become increasingly evident that detailed measurements of the aerodynamic characteristics of Prop-Fan blades are required to understand the specific nature of Prop-Fan blade flows. Such flows are complicated, containing features such as three dimensional boundary layer effects, leading and tip edge vortices, and shock waves. They are therefore not easily predicted. However, an understanding of the specific nature of Prop-Fan blade flows is vital to the process of refining design methodologies and to improving the performance of new Prop-Fan designs.

The need for measured Prop-Fan blade aerodynamic data has prompted NASA and Hamilton Standard to pursue a program of wind tunnel experiments where both steady and unsteady blade surface pressure measurements would be made. Reporting of the steady pressure experiment has been done in Reference 1. The analysis of the unsteady blade surface pressure testing that was carried out under the program in March of 1987 is reported here. Experimental methods, measured data, and some preliminary comments on observed aerodynamic features are discussed.

SR-7L PROP-FAN DESCRIPTION

The SR-7L Large Scale Advanced Prop-Fan, illustrated in Figure 1, is a 2.74 meter (9 foot) diameter, eight bladed tractor configuration which was designed for 0.85 Mach number cruise speed at an altitude of 10,667 meters (35,000 feet), ISA. The SR-7L Prop-Fan was designed for high efficiency and low noise while maintaining the necessary restrictions on blade stress, stability and frequency characteristics. Additional fundamental design point parameters are:

Disc loading (Power/diameter^2)	259.6 kW/m^2	(32 shp/ft^2)
Tip speed	243.8 m/s	(800 ft/s)
Advance ratio	3.06	
Power coefficient	1.448	
Activity factor per blade	227.3	
Integrated design lift coeff.	0.191	

Rotation of the Prop-Fan is counterclockwise as viewed from the rear looking forward. The hub to tip ratio is 0.24, and the blades incorporate NACA Series 65/CA airfoils from the root to the 36% radius and NACA Series 16 airfoils from the 52% radius to the tip, with "transition" airfoils in the remaining, middle, portion of the blade. The blade's mid-chord line sweeps back to a maximum of 36° at the tip station. Additional information on the SR-7L Prop-Fan design can be found in Reference 2.

TEST FACILITIES AND EXPERIMENTAL APPARATUS

Wind Tunnel

The blade unsteady surface pressure test was conducted in the 47 m^2 (506 ft^2) atmospheric test section of the ONERA S1-MA wind tunnel in Modane, France.

Prop-Fan drive power was supplied by two gas turbine engines which were located approximately 5 meters (16.4 feet) downstream of the rotor plane. The power [1000 kW (1341 hp), maximum] was transmitted to the rotor through a series of mechanical couplings.

Diagrams of the wind tunnel and the test section with the uniform inflow Prop-Fan installation are shown in Figure 2. Note that the wind tunnel test section is unsymmetrical and the tunnel and Prop-Fan axes were not coincident.

The wind tunnel stagnation conditions were measured in a settling chamber located upstream of the test section. The tunnel static pressure was measured on the wall of the test section in the Prop-Fan plane of rotation and was corrected according to flow survey data to provide the upstream static pressure for undisturbed inflow. The flow survey data were acquired, during testing for Hamilton Standard in 1986, by probing the flow field pressures parallel to the Prop-Fan axis and then subtracting theoretical body flow field effects.

With the tunnel static pressure and stagnation conditions known, the inflow Mach number and static temperature were determined from the one dimensional compressible flow functions.

Prop-Fan Test Installation

The Prop-Fan was operated in a two bladed configuration as shown in Figure 3. This configuration was necessitated by limitations in power available from the drive engines. By running the system with two blades, full and over design power loading conditions were attainable on a per blade basis for inflow Mach numbers through 0.50.

The three test configurations as installed in the wind tunnel are shown in Figure 4. The Prop-Fan support apparatus consisted of a cable and rod system which was designed and tested to assure adequate system damping and structural integrity. It should be noted that the Prop-Fan was "pitched up" by 3 degrees during the angular inflow testing.

Prop-Fan drive power and blade angle were remotely controlled by test personnel in a room adjacent to the wind tunnel test section. Blade angle measurements were made using a potentiometer system.

Wake Generator Post

The cylindrical wake generator post was used to produce a narrow inflow disturbance which the instrumented blade would experience twice per revolution. The post was 0.102 m (4.00 in) in diameter and was mounted vertically on the Prop-Fan center-line at a distance of one rotor radius upstream of the rotor plane.

The range of Reynolds numbers (based on cylinder diameter) was 2.2×10^4 to 1.5×10^5 for inflow Mach numbers from 0.01 to 0.70; note that this range covers the regime where Karman vortex streets occur ($50 < Re < 4 \times 10^5$) and where turbulent separation occurs ($Re > 4 \times 10^5$) as defined in Reference 3.

Instrumented Blade

Collection of the blade surface unsteady pressure data was accomplished with the instrumented SR-7L blade shown in Figure 5. The blade was configured with two radial stations of pressure transducers on both pressure and suction sides. The locations and labeling scheme for the transducers are shown in Figure 6.

The blade was fabricated with a 0.89 mm (0.035 in) thick plastic skin layer on each side. The purpose of the skin was to provide room for flush mounting the transducers and routing the lead wires along the blade surfaces without disrupting the blade internal structure and also maintaining a smooth blade surface. Cross sectional and plan views of the transducer and lead wire installations in the plastic skin are shown in Figure 7.

Utilization of the skin cladding approach described above resulted in an increase in blade thickness of 1.78 ±0.25 mm (0.070 ±0.010 in) from the design thickness. This amounts to a 10.4 ±1.5% increase in the airfoil section thickness ratio (mid chord thickness/chord) at the inboard radial station and a 27.6 ±3.9% increase at the outboard radial station. A leading edge fiberglass wrap which was used to lock the plastic skins in place resulted in a 0.76 ±0.18 mm (0.030 ±0.007 in) increase in the leading edge radii. The transition from the leading edge radii to the airfoil surfaces was smooth.

Pressure Transducers and Instrumentation

A general schematic of the LAP instrumentation system can be seen in Figure 8. The LAP dynamic pressure blade was instrumented with twenty-six pressure transducers and four strain gages. Signal conditioning and strain gage bridge completion were provided by a printed circuit board located in the cuff of the blade. Programmable connector sockets were used as an interface between the signal conditioning boards and the rotating interface board (RIB).

As shown in Figure 8, the RIB board provided signal and power interconnection between components of the rotating system. All signals from the programmable connector were routed through the RIB board to the VCO cases. Each VCO case contained 16 VCO's (IRIG channels 1A-16A) and a line driver/mixing amplifier. The output of each VCO case was a 16 channel FM frequency multiplexed signal which was transmitted to the non-rotating instrumentation via a pair of slip rings. This system, therefore, could handle up to 32 active channels. The typical measurement uncertainty of the system was less than ±5 percent.

The LAP dynamic pressure blade was instrumented with 26 (13 on each side) Endevco model 8515A 15SM2 pressure transducers. (See Figure 9.) These were sealed gages with a pressure range of ±69 KPa (±10 psi). Resistor R1 (1,000 OHM) provided improved temperature compensation and an attenuation resistor R2 (500 OHM) reduced transducer output. Elastomer mounting was used to isolate the transducer from the blade to reduce base strain sensitivity.

The signal conditioning board, mounted in the cuff of the dynamic pressure blade, provided three functions: 1) Pressure transducer to instrumentation interface, 2) Strain gage bridge completion (not shown in Figure 9), and 3) Shunt CAL for each strain gage bridge (not shown in Figure 9).

The unsteady pressure instrumentation utilized two identical voltage controlled oscillator (VCO) cases each containing 16 VCO's and matching preamplifiers and one mixing amplifier/line driver. Each VCO consisted of both a preamplifier (Low Level Amplifier) and VCO module which were matched in pairs. The preamplifiers had a standard fixed gain of 250 ±2% to accommodate conditioned pressure and strain gage signals. The VCO subcarrier frequencies were all standard IRIG A constant bandwidth (CBW) channels (1A-16A) with a deviation of ±2 KHz. All 16 VCO outputs in each case were mixed into a single 16 channel frequency multiplexed signal.

A rotating power supply provided +5 VDC excitation for the pressure transducers and strain gages and supplied the 25.5 VDC power required for the rotating electronics. It derived its power through slip rings from the primary power supply located on the non-rotating side. The primary power supply output voltage could be set by the user at one of three levels. This level was sensed by the rotating power supply and forced into one of three possible modes - the USE, FULL SCALE STANDARDIZE (for strain gages only) or the ZERO mode. This feature allowed the transmission of the standardizing commands to the rotating electronics using a minimum number of slip-rings.

The LAP instrumentation slip ring was an eight-ring platter-type assembly which provided the electrical interface for the propeller measurements between the rotating propeller assembly and the non-rotating propeller control. Five of the eight rings were used for the dynamic pressure instrumentation as shown in Figure 9.

Each of the two detranslators accepted a 16 channel VCO case output. The detranslator, utilizing a filtering and heterodyning process, converted the multiplex signal into four groups with four subcarriers each. These subcarriers were IRIG channels 1A, 2A, 3A and 4A in all cases. A total of eight multiplex groups originated at the detranslators and were recorded directly on tape.

TEST PROCEDURE AND OPERATING CONDITIONS

The ranges of operating conditions that were run for the three test installations are given in Table 1. The table is ordered by increasing Mach number and subordered by increasing power coefficient. The point numbers, given at the left in the table, refer to the operating condition numbers specified in the test plan (Reference 4). The measurement uncertainties for the operating parameters are indicated by the $\pm$ signs. Additional data containing tunnel operating parameters can be found in Appendix D.

The basic format of the experiment follows Table 1; the 3° angular inflow case was run first followed by the wake and uniform inflow cases. For each of the cases the Prop-Fan was stepped through the test points and data were acquired during a 2 to 3 minute hold at each point.

In general, the procedure for setting a specific test point was to set inflow Mach number and then adjust the rotor speed and blade angle, to obtain a desired power coefficient. This procedure assured good power coefficient matches for the three test installations and resulted in minimal variation of Mach number and advance ratio.

Test points 2, 3 and 4 in Table 1 approximate static propeller conditions of increasing power, and test points 5, 5A, 5B and 6 were selected to investigate takeoff conditions. The three runs at 0.50 inflow Mach number cover a wide range of power loading conditions and include a case at the design cruise power coefficient per blade. Points 10 and 11 were run only for the angular inflow testing since it was determined that the pressure transducers were too susceptible to damage at high inflow speeds.

DATA REDUCTION

Fourier Analysis

The objective of the data reduction process was to express the periodic pressure signals (relative to blade surface static pressure) in Fourier coefficient form. This allowed the data to be presented as a compact tabulation of signal harmonics of blade rotational frequency, from which one may reconstruct the original pressure waveforms with resolution corresponding to the number of harmonics given.

Prior to analysis, a particular data signal was low-pass filtered at 1000 Hz to eliminate high frequency noise (the limit of the data aquisition system was 1000 Hz, so no loss of data occurred during this process).

The Fourier coefficients were obtained by using the once-per-revolution pip signal to divide the continuous pressure signals into a series of 1024 waveforms, each with period corresponding to one revolution of the rotor. A digital Fourier transform analyzer was then used to obtain the first 35 Fourier coefficients of each waveform. Average values of the coefficients were then determined from the 1024 waveforms sampled.

Definitions of the Fourier coefficients, determined in this way, are:

$$a_k = \frac{1}{L}\sum_{\ell=1}^{L}\frac{1}{N}\sum_{n=1}^{N} p(n,\ell)\,\cos(2\pi kn/N) \qquad (1)$$

$$b_k = \frac{1}{L}\sum_{\ell=1}^{L}\frac{1}{N}\sum_{n=1}^{N} p(n,\ell)\,\sin(2\pi kn/N) \qquad (2)$$

where $k = 1,2,\ldots,K$ (K=35) is the harmonic of blade rotational frequency

$n = 1,2,\ldots,N$ (N) is the sample index,

$\ell = 1,2,\ldots,L$ (L=1024) is the revolution number,

and $p(n,\ell)$ is the unsteady pressure (relative to the mean blade surface pressure) for sample n in revolution ℓ.

The Fourier representation of the average waveform may then be obtained as a function of blade azimuth angle θ, by

$$P(\theta) = \sum_{k=1}^{K} a_k \cos(\theta k) + b_k \sin(\theta k) \qquad (3)$$

The amplitude of the k^{th} harmonic is $(a_k^2 + b_k^2)^{1/2}$.

In Equation 3, $\theta = 0°$ corresponds to the angular position of the once per revolution pip signal (116° before top-dead-center). Plots, which are discussed later in the report are given such that 0° corresponds to top-dead-center.

Correction for Non-uniformities in the Tunnel Flow

Upon review of the data, reduced as described above, some small (but significant) unsteady pressure response was found in the nominally uniform inflow data. This response was primarily of the first harmonic order, but some higher order response was exhibited as well. It is believed that the principal cause of this response was residual flow angularity resulting from the tunnel section asymmetry mentioned above.

In order to correct the angular and wake inflow spectra for residual flow angularity, the Fourier coefficients from each transducer and run number for the angular and wake inflow data were modified by subtracting the components from the corresponding uniform inflow case. That is,

$$a_k(i,j)_{\substack{\text{angular}\\\text{or wake}}}^{\text{corrected}} = a_k(i,j)_{\substack{\text{angular}\\\text{or wake}}} - a_k(i,j)_{\text{uniform}} \qquad (4)$$

where $k = 1,2,\ldots,35$ and i and j are the pressure transducer and, run numbers, respectively. The corresponding corrections were also made to the b_k's.

This correction was applied to every case for which corresponding uniform inflow data was available. Table 2 shows the status of the data; angular and wake inflow data signals marked "X" have been corrected; signals marked "*" were not corrected.

RESULTS AND DISCUSSION

Format of Data Presented

The uniform flow, angular flow, and wake data tabulations can be found in Appendices A through C, respectively. The data in each appendix are ordered in the same way as previously explained for Tables 1 and 2. Each page contains the data in terms of a_k, b_k and the corresponding component amplitudes. Also included are the wind tunnel/Prop-Fan operating conditions and the location of a given pressure transducer on the blade.

General Information About the Data

Throughout the testing some of the pressure transducers were inoperable due to intermittent signals in the system instrumentation. This left some gaps in the data. However, the existing data are adequate to provide an understanding of unsteady blade surface pressure behavior. The appendices include only data from functioning transducers.

Signal levels for the low power and the low speed conditions were quite low and noise contamination was observed in some of the signals. The random part of the noise was reduced by averaging the signals over 1024 revolutions. This enhances the repetitive portion of the signal while suppressing the random part. However, in some instances the noise occurred at harmonics of the blade's rotational frequency. In these cases the noise was not averaged out and is included in the Fourier coefficients presented in the tables.

Data Representation - Waveform Versus Fourier Components

Data are represented as complex Fourier coefficients for 35 harmonics of rotational frequency. To determine how well 35 harmonics represent the measured waveform, an inverse transform was performed for both a representative angular inflow condition and a wake condition. Shown in Figure 10 is a comparison of the measured and re-computed waveforms of the angular inflow and wake conditions. It can be seen that, for the angular inflow condition, 35 harmonics adequately represent the waveform. In the wake inflow case, it can be seen that the waveform is generally represented well with 35 harmonics. However, the sharp peaks of the re-computed waveforms are slightly lower in amplitude than those of the measured waveforms. This indicates that small amounts of additional upper harmonic content are present.

The Fourier analysis of the data appears to provide some low-pass filtering of the data. However, it should be emphasized that the instrumentation limitations of the data acquisition system was 1000 Hz which is approximately equal to the frequency represented by 35 harmonics of rotational frequency.

Waveform and Spectrum Examples

To provide an illustration of the data collected during the test in waveform and spectrum content, examples are given in Figure 11 that show periodic variations in pressure and corresponding frequency spectra. The operating point shown is representative of the Prop-Fan takeoff condition blade surface pressures on the suction side of the blade at approximately mid-chord and 90% blade radius.

The pressure versus time plots shows the average variation in pressure the blade experienced on a circumferential basis during 1024 revolutions. This tends to average out the non-repetitive portion of the waveform. The spectra shown were obtained by Fourier transforming the signal with a 4.8 second averaging time. The frequency bandwidth for these spectra is 1.25 Hz.

Discussion of Representative Data

The data selected for discussion are representative of cruise and takeoff conditions. The conditions chosen are as follows:

CONDITION REPRESENTED	RUN	TEST POINT	TUNNEL MACH NO. M_∞	ADVANCE RATIO J	POWER COEFF. Cp	INFLOW CONDITION
CRUISE	38	8	0.500	3.064	0.360	UNIFORM
CRUISE	10	8	0.501	3.065	0.363	ANGULAR
CRUISE	29	8	0.500	3.063	0.361	WAKE
TAKEOFF	8	6	0.199	0.881	0.251	ANGULAR
TAKEOFF	25	6	0.199	0.880	0.250	WAKE

It should be noted that although M_∞ is not equal to the 0.8 M_∞ of the design cruise condition, the advance ratio (J) and power coefficient (Cp) on a per blade basis equal the cruise values so that the non-dimensional loading and flow angles are approximately preserved.

An example of the unsteady blade response in uniform flow can be seen in Figure 12. The point shown is approximately at mid-chord of the outboard radial station (r/R = 0.91) on the suction (or camber) side of the blade. It can be seen that the pressure is reasonably uniform, with only minor variations. The uniform pressure indicates that the inflow is reasonably uniform in the tunnel. This is typical of the magnitude of the "non-uniformity" in the uniform flow data at other pressure transducers.

The wake and angular inflow data are presented in Figures 13 through 28. Each of the figures present the data on one side of the blade (suction or pressure) at one radial station (r/R = 0.64 or r/R = 0.91). Each figure shows how the blade surface pressure varies as a function of azimuth and chordwise location. The first waveform shown on each figure is the operating transducer closest to the leading edge with subsequent waveforms representing pressure response progressing toward the trailing edge. In all cases the waveforms are those computed from the 35 Fourier coefficients.

In Figure 13 the waveforms are shown on the pressure side of the blade at r/R = 0.64 for an angular inflow cruise condition. The sinusoidal response is typical of that expected for propellers operating at angle of attack. It can be seen that the blade has the largest response slightly downstream from the leading edge and has progressively less response toward the trailing edge. The once-per-revolution response is clearly evident. Shown in Figure 14 are the pressure waveforms for the suction (camber) side of the blade at r/R = 0.64. It can be seen that response on the suction side is similar to that on the pressure side with the exception of the point closest to the leading edge. At the x/c = .049 location there appears to be some additional response around 45 and 180 degrees. The cause of this is not known at this time. Shown in Figures 15 and 16 are the blade pressures for the pressure and suction sides at r/R = 0.91. It can be seen that results at this radial station are similar to those observed at the 0.64 r/R radial locations.

Figures 17 and 18 present cruise condition wake inflow comparisons on the pressure and suction blade sides at r/R = 0.64. The wake is fairly broad but can clearly be seen to occur twice-per-revolution at 0 and 180 degrees. In Figures 19 and 20 (r/R = 0.91) the wake cannot be seen as clearly at 0 and 180 degrees. Some additional response can be seen at other azimuth locations that are equal to or greater than the magnitude of the wake response.

Figures 21 and 22 show results at takeoff conditions with angular inflow on the pressure and suction sides of the blades at r/R = 0.64. It can be seen that very little response occurs on the pressure side of the blade. On the suction side of the blade the response is non-sinusoidal. This may be indicative of non-linear response and could be due to a leading-edge vortex that is just beginning to form at this location. (The r/R = 0.64 location is just past the "knee" of the blade where the blade starts to sweep back.) The leading edge vortex phenomenon has been observed in high power cases as reported in Reference 1. At the tip location (r/R = 0.91) a similar phenomenon appears to occur as shown in Figures 23 and 24. The pressure side of the blade shows sinusoidal response across the blade chord. However, on the suction side of the blade, non-linear response is present.

Shown in Figures 25 through 28 are the waveforms seen at at takeoff condition with a wake inflow at r/R = 0.64 and r/R = 0.91 on the blade pressure and suction surfaces. It can been seen at both radial stations that the pressure side of the blade has little response to the incoming wake. However, the suction side of the blade responds more strongly. The increased response may be due to the motion of leading edge and tip vortices on the suction surface caused by periodic angle-of-attack variations.

CONCLUSIONS

- Unsteady blade surface pressure data were successfully collected over the following range of conditions:

Angular Inflow (3°)	$0.02 \leq M_\infty \leq 0.70$
Wake Inflow	$0.03 \leq M_\infty \leq 0.50$
Uniform Inflow (0°)	$0.02 \leq M_\infty \leq 0.50$

- Presenting the data in Fourier coefficient form for the first 35 harmonics of rotational frequency provided a good representation of the data in a compact tabular form. This technique allowed the small non-uniformities of the tunnel to be "corrected out" of the angular and wake inflow data.

- The uniform inflow data shows some traces of distortion. This is probably due to tunnel asymmetry.

- Unsteady pressure response is evident in the angular inflow and wake data. The angular inflow data clearly shows a dominant once-per-revolution response while the wake data shows response twice-per-revolution as the instrumented blade passes the wake generating post.

- Sinusoidal response was observed on the pressure (face) side of the blade in all cases examined for angular inflow conditions.

- Sinusoidal response was observed on the suction (camber) side of the blade under low loading conditions. However, under high loading conditions a non-sinusoidal response was observed. The non-sinusoidal response may be due to leading edge and tip vortices that distort the response. Another possibility is the formation and breakdown of the vortices as the angular inflow or wake inflow modulates the angle-of-attack.

SYMBOLS AND ABBREVIATIONS

a_K	-	Real part of Fourier coefficient of "K^{th}" harmonic
b_K	-	Imaginary part of Fourier coefficient of "K^{th}" harmonic
C	-	Blade chord
CBW	-	Constant Bandwidth
c_p	-	Power coefficient = (Power absorbed)/$\rho(2\pi\Omega)^3(2R)^5$
FM	-	Frequency modulation
hp	-	Horse power
i	-	Pressure transducer number
j	-	Point number
J	-	Advance ratio $\pi M_x/M_t$
K	-	Harmonic of blade rotational frequency
KPa	-	Kilo Pascals
KW	-	Kilowatts
ℓ	-	Revolution number
LE	-	Leading edge
m	-	Meters
M_∞	-	Inflow Mach number
M_t	-	Tip Mach number
n	-	Sample index number
$P(n,\ell)$	-	Unsteady pressure for sample n in revolution ℓ
PSI	-	Pressure (lb/inch^2)
PT	-	Pressure Transducer
r	-	Radial distance from hub center-line
R	-	Rotor radius

SYMBOLS AND ABBREVIATIONS (Continued)

Re	-	Reynolds number
RIB	-	Rotating interface board
TE	-	Trailing edge
VCO	-	Voltage controlled oscillator
VDC	-	Voltage (direct current)
X/C	-	Non-dimensional blade chord (distance from LE)
β	-	Blade angle at r = 104.1 cm (degrees)
Ω	-	Rotor speed, radians/second
ρ	-	Air density Kg/m^3 (lb/ft^3)

REFERENCES

1. Bushnell, P., "Measurement of the Steady Surface Pressure Distribution on a Single Rotation Large Scale Advanced Prop-Fan Blade of Mach numbers from 0.03 to 0.78", NASA Lewis Contract NAS3-23051, October 1987.

2. Sullivan, W., Turnberg, J., Violette, J., "Large-Scale Advanced Prop-Fan (LAP) Blade Design", NASA Lewis Contract NAS3-23051, NASA CR-174790, October 3, 1985.

3. Kuthe, A. M., Chow, C. Y., "Foundations of Aerodynamics: Bases of Aerodynamic Design", 3d ed., John Wiley & Sons, New York, 1976.

4. Plan of Test 267X-135 Rev. D dated 12/5/86.

Table 1

Operating Conditions for 3° Angular Inflow

Point Number	Mach Number, M_∞	Advance Ratio, J	Power coeff., CP	Blade Angle, β
2	0.017 ±0.013	0.107 ±0.076	0.096 ±0.001	14.9 ±0.5°
3	0.026 ±0.013	0.159 ±0.079	0.155 ±0.001	19.1 ±0.5°
4	0.030 ±0.013	0.186 ±0.079	0.204 ±0.001	22.1 ±0.5°
5	0.200 ±0.003	0.883 ±0.015	0.101 ±0.001	26.0 ±0.5°
5A	0.200 ±0.003	0.879 ±0.015	0.149 ±0.001	27.2 ±0.5°
5B	0.200 ±0.003	0.881 ±0.015	0.200 ±0.001	29.5 ±0.5°
6	0.199 ±0.003	0.881 ±0.015	0.251 ±0.001	31.6 ±0.5°
9	0.500 ±0.002	3.070 ±0.012	0.112 ±0.001	52.0 ±0.5°
8	0.500 ±0.002	3.063 ±0.012	0.361 ±0.002	55.5 ±0.5°
7	0.500 ±0.002	3.065 ±0.012	0.649 ±0.003	59.4 ±0.5°
10	0.598 ±0.001	3.065 ±0.010	0.226 ±0.001	53.9 ±0.5°
11	0.700 ±0.001	3.058 ±0.008	0.216 ±0.001	53.9 ±0.5°

Operating Conditions for Inflow with Wake

Point Number	Mach Number, M_∞	Advance Ratio, J	Power coeff., CP	Blade Angle, β
4	0.029 ±0.013	0.177 ±0.079	0.204 ±0.001	22.2 ±0.5°
5	0.200 ±0.003	0.884 ±0.015	0.101 ±0.001	26.0 ±0.5°
5A	0.199 ±0.003	0.883 ±0.015	0.151 ±0.001	27.4 ±0.5°
5B	0.199 ±0.003	0.881 ±0.015	0.202 ±0.001	29.7 ±0.5°
6	0.199 ±0.003	0.880 ±0.015	0.250 ±0.001	31.6 ±0.5°
9	0.500 ±0.002	3.063 ±0.012	0.114 ±0.001	51.9 ±0.5°
8	0.501 ±0.002	3.065 ±0.012	0.363 ±0.002	54.9 ±0.5°
7	0.501 ±0.002	3.067 ±0.012	0.650 ±0.003	58.4 ±0.5°

Operating Conditions for Uniform Inflow

Point Number	Mach Number, M_∞	Advance Ratio, J	Power coeff., CP	Blade Angle, β
4	0.022 ±0.013	0.138 ±0.079	0.208 ±0.001	22.2 ±0.5°
5	0.201 ±0.003	0.881 ±0.015	0.100 ±0.001	26.0 ±0.5°
5A	0.200 ±0.003	0.883 ±0.015	0.152 ±0.001	28.2 ±0.5°
5B	0.200 ±0.003	0.882 ±0.015	0.201 ±0.001	29.8 ±0.5°
6	0.199 ±0.003	0.880 ±0.015	0.249 ±0.001	32.3 ±0.5°
9	0.500 ±0.002	3.068 ±0.012	0.109 ±0.001	52.3 ±0.5°
8	0.500 ±0.002	3.064 ±0.012	0.360 ±0.002	55.5 ±0.5°
7	0.499 ±0.002	3.065 ±0.012	0.653 ±0.003	58.5 ±0.5°

Table 2

SR7 BLADE - UNSTEADY PRESSURE DATA

PRESSURE TRANSDUCERS (PT'S) WITH USABLE SIGNALS
VERSUS RUN AND POINT NUMBERS

A - ANGULAR INFLOW
W - WAKE INFLOW
U - UNIFORM INFLOW

X - USABLE DATA; ANGULAR AND WAKE INFLOW DATA CORRECTED FOR RESIDUAL UNSTEADY REPONSE OF THE CORRESPONDING UNIFORM INFLOW DATA.

* - USABLE DATA; NO CORRECTION.

POINT	2	3	4		5		5A		5B		6			9			8			7			10	11
RUN A	2	3	4		5		6		7		8			9			10			11			12	13
W			20		21		28		23		25			26			29			30				
U				32		33		34		35		36			37			38			39			
PT 1																								
2	*	*	X	X	X	X	X	X	X	X	X	X	X	X	X	X	X	X	X	X	X	*		
3																								
4																								
5		*	*		*		X	X	X	X	X	X	X	X	X	X	X	X	X	X	X	*		
6		*	X	X	X	X	X	X	X	X	X	X	X	X	X	X	X	X	X	X	X	*		
7							*		*		*	*		*			*			*		*		
8					X	X	X	X	X	X	X	X	X	X	X	X	X	X	X	X	X	*	*	
9					X	X	X							X	X	X	X	X	X	X	X	*		
10				X	X	X	X	X	X	X	X	X	X	X	X	X	X	X	X	X	X	*		
11					*		X	X	X	X	X	X		X	X	X	X	X	X	X	X	*		
12			*		X	X	X	X	X	X	X	X		X	X	X	X	X	X	X	X	*		
13					X	X	X	X	X	X	X	X		X	X	X	X	X	X	X	X	*		
14																								
15											X	X	X	X	X	X	X	X	X	X	X	*		
16			X	X	X	X	X	X	X	X	X	X	X	X	X	X	X	X	X	X	X	*		
17																								
18			*		*				*		*			*			*			*		*		
19																								
20			X	X	X	X	X	X	X	X	X	X	X	X	X	X	X	X	X	X	X	*	*	
21	*	*	*		*		*		*		*													
22																								
23	*	*	*		*		X	X	X	X	X	X	X	X	X	X	X	X	X	X	X			
24	*	*	*		*		X	X	X	X	X	X	X	X	X	X	X	X	X	X	X			
25	*	*	*		*		X	X	X	X	X	X	X	X	X	X	X	X	X	X	X			
26	*	*	*		*		X	X	X	X	X	X	X	X	X	X	X	X	X	X	X			

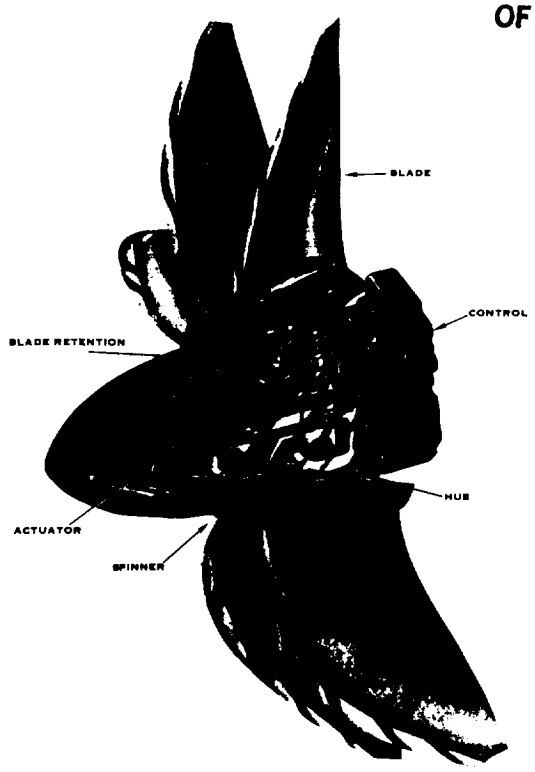

FIGURE 1. - LARGE SCALE ADVANCED PROP-FAN.

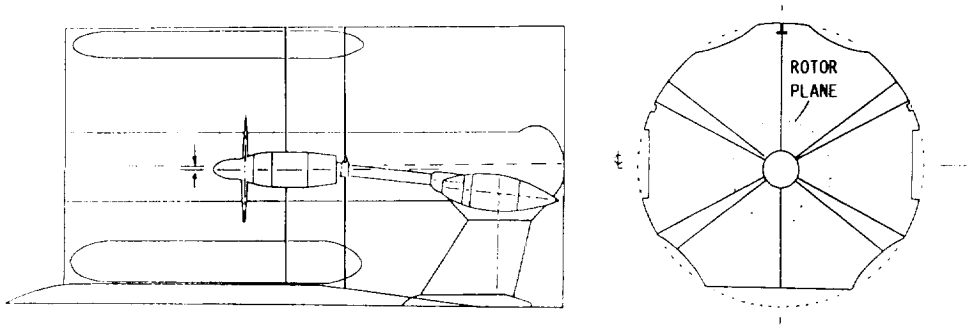

FIGURE 2. - SR7 PROPFAN INSTALLATION IN S1-MA TRANSONIC TEST SECTION (UNIFORM INFLOW).

FIGURE 3. - PROPFAN UNSTEADY PRESSURE TEST SETUP.

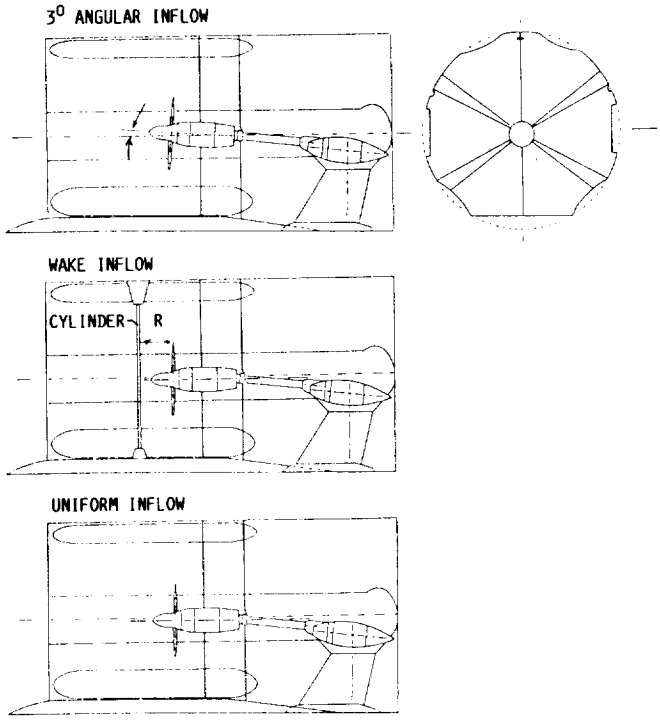

FIGURE 4. - TEST CONFIGURATION FOR 3⁰ ANGULAR, WAKE AND UNIFORM INFLOW.

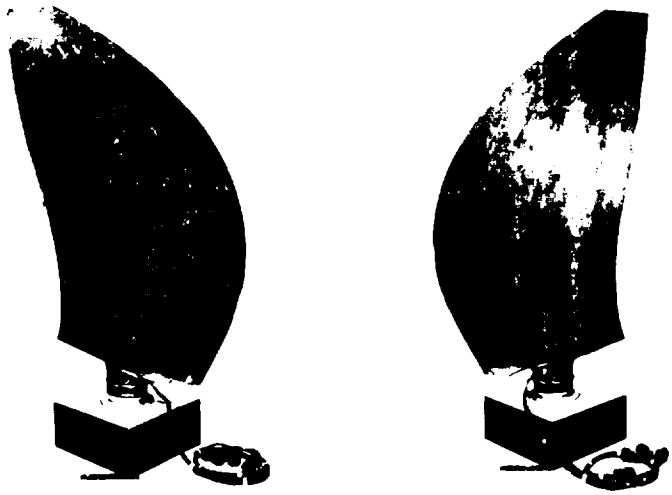

FIGURE 5. - LAP UNSTEADY PRESSURE BLADE.

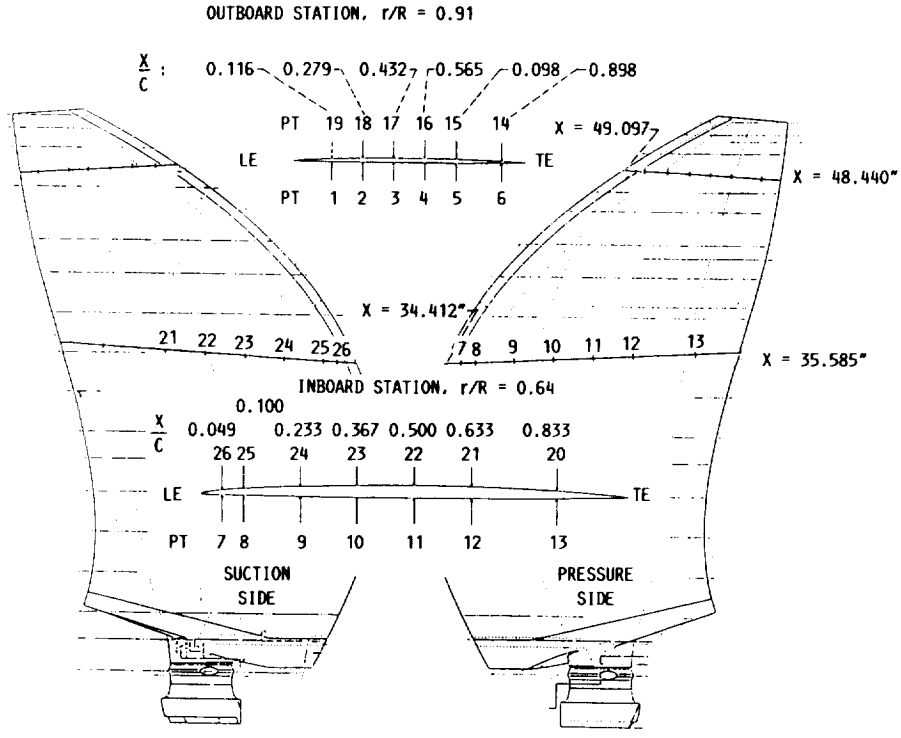

FIGURE 6. - SR7 UNSTEADY PRESSURE INSTRUMENTED BLADE - TRANSDUCER LOCATIONS AND NUMBERING.

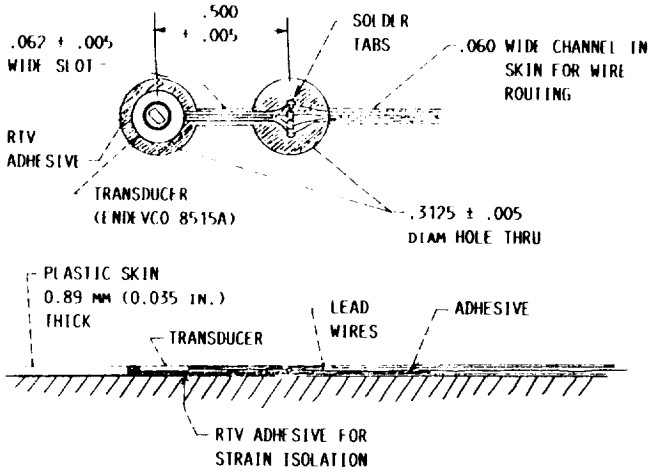

FIGURE 7. - PRESSURE TRANSDUCER INSTALLATION.

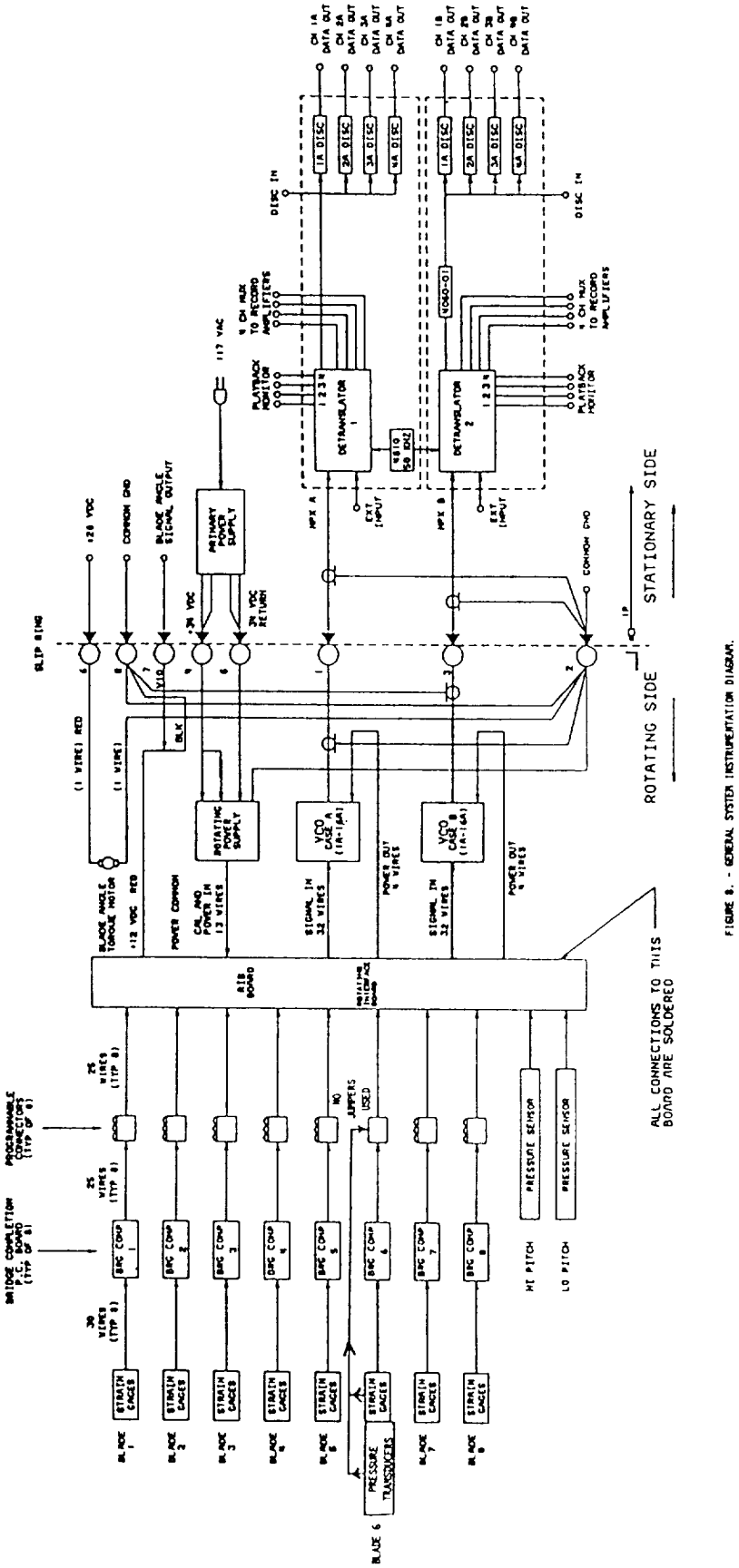

FIGURE 8. - GENERAL SYSTEM INSTRUMENTATION DIAGRAM.

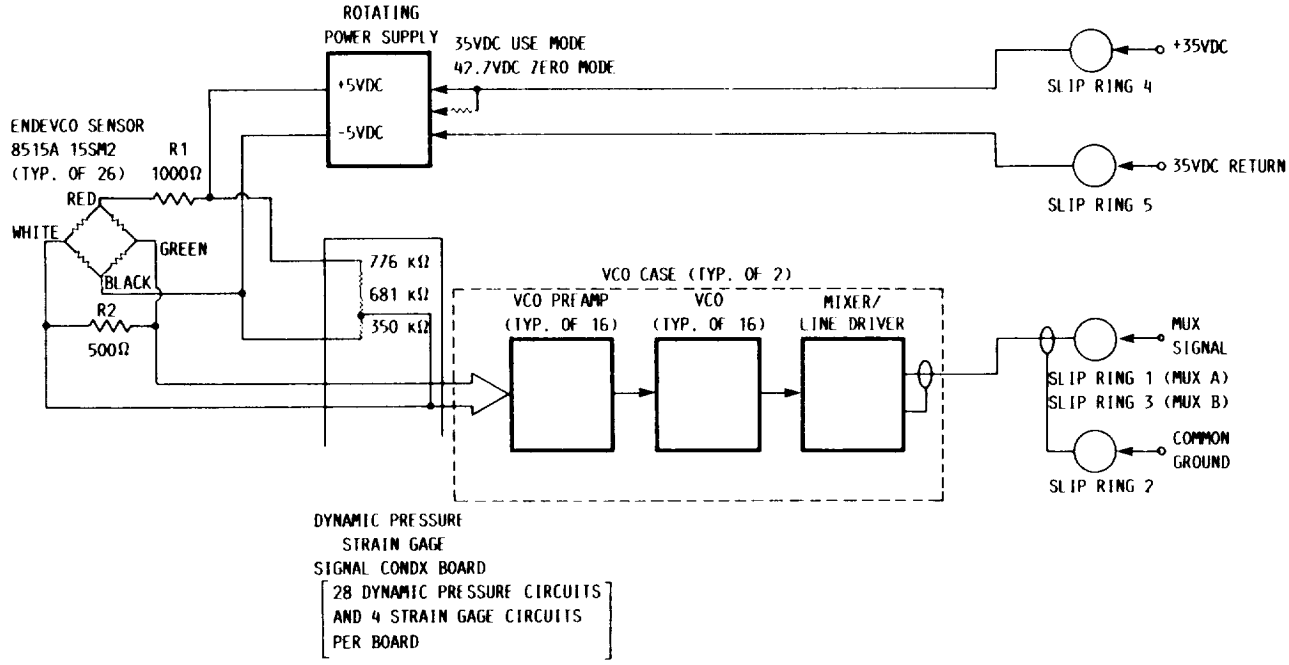

FIGURE 9. - ROTATING DYNAMIC PRESSURE INSTRUMENTATION.

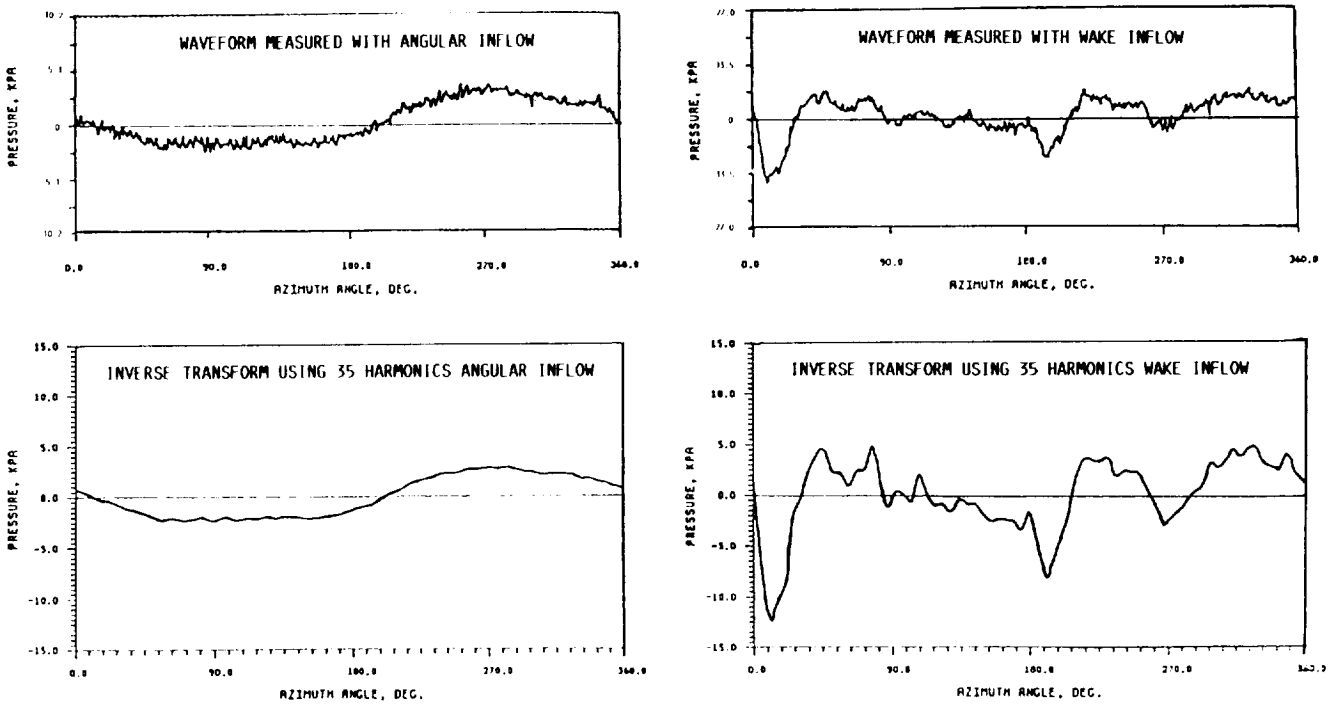

FIGURE 10. - COMPARISON OF MEASURED AND RE-CALCULATED WAVEFORMS OF UNSTEADY BLADE SURFACE PRESSURE.

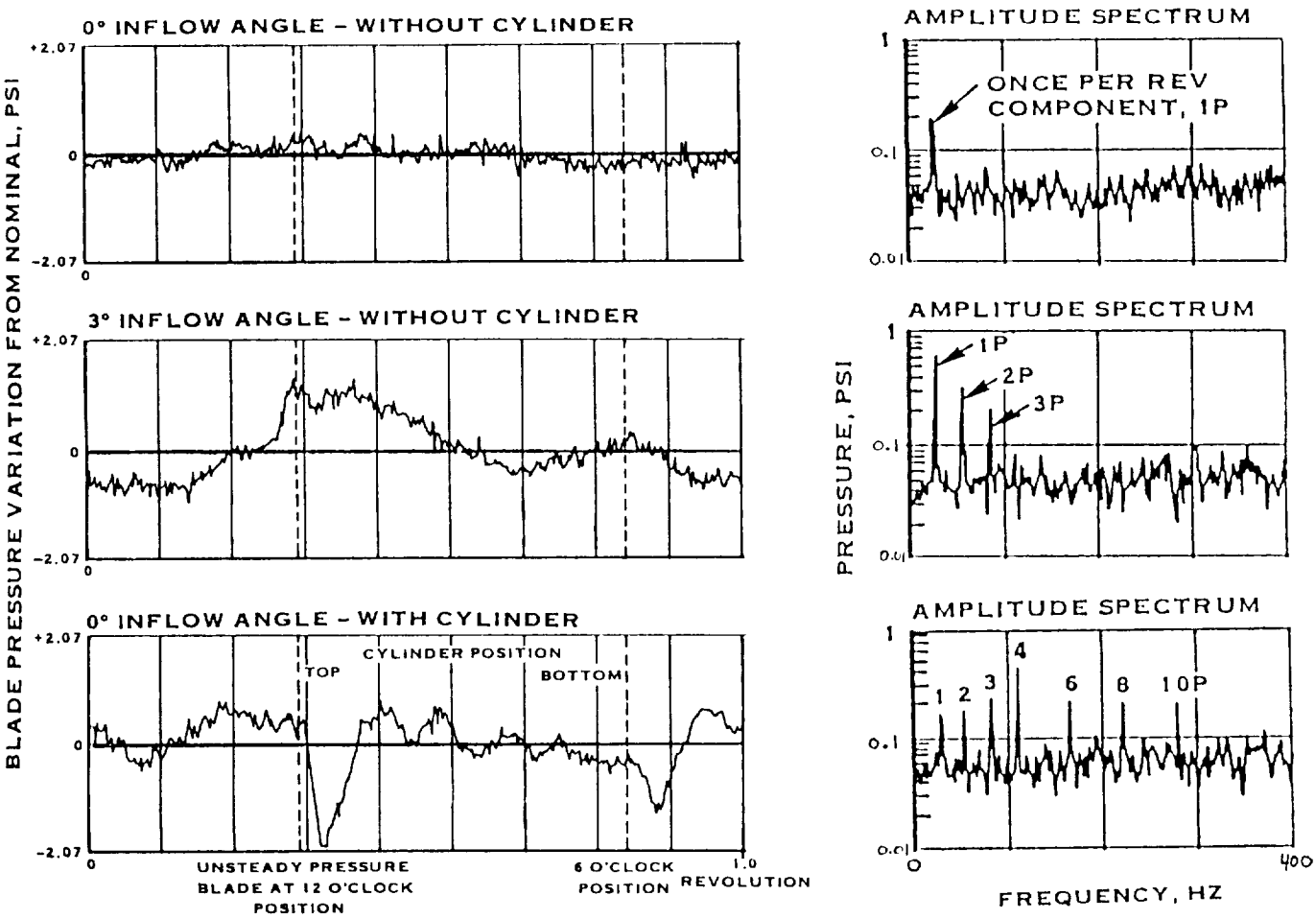

(Mn = 0.2, J = 0.883, Cp = 0.250, β3/4 = 32°)

FIGURE 11. - TYPICAL WAVEFORMS AND SPECTRA OF LAP UNSTEADY BLADE SURFACE PRESSURE MEASUREMENTS.

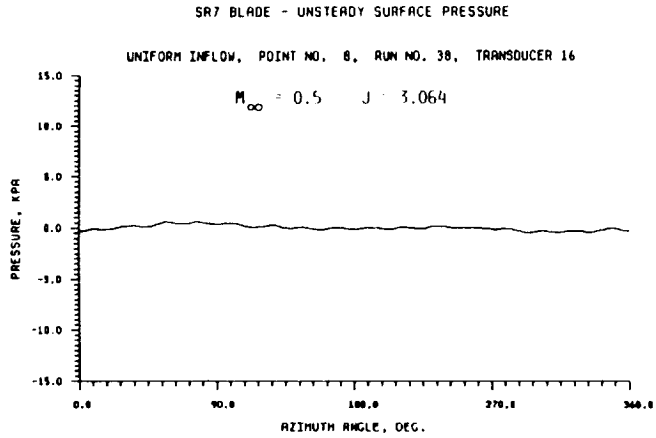

FIGURE 12. TYPICAL BLADE SURFACE PRESSURE VARIATION WITH AZIMUTHAL LOCATION WITH "UNIFORM" INFLOW.

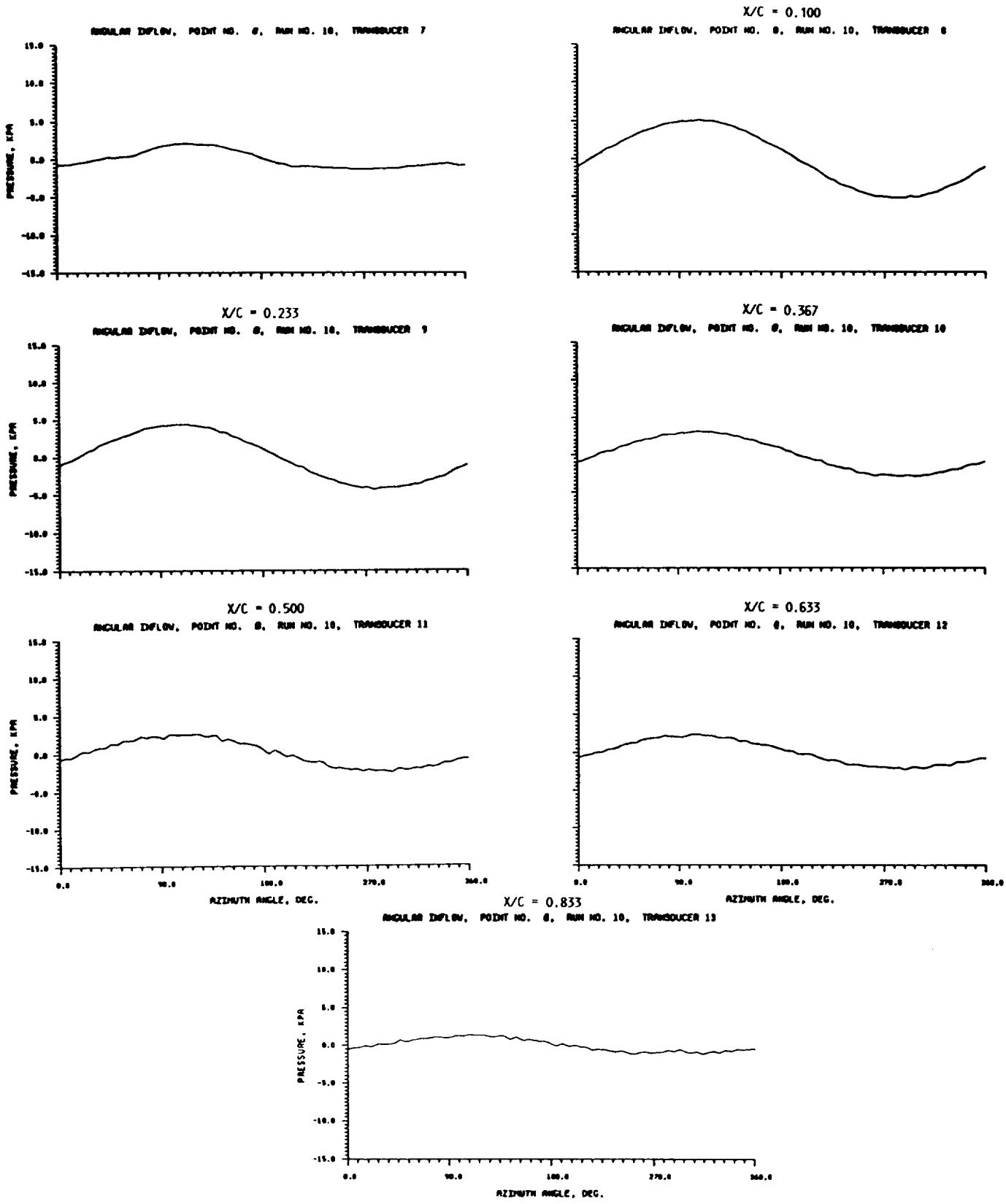

FIGURE 13. - BLADE SURFACE PRESSURE AS FUNCTION OF AZIMUTH LOCATION FOR CRUISE CONDITION WITH ANGULAR INFLOW.

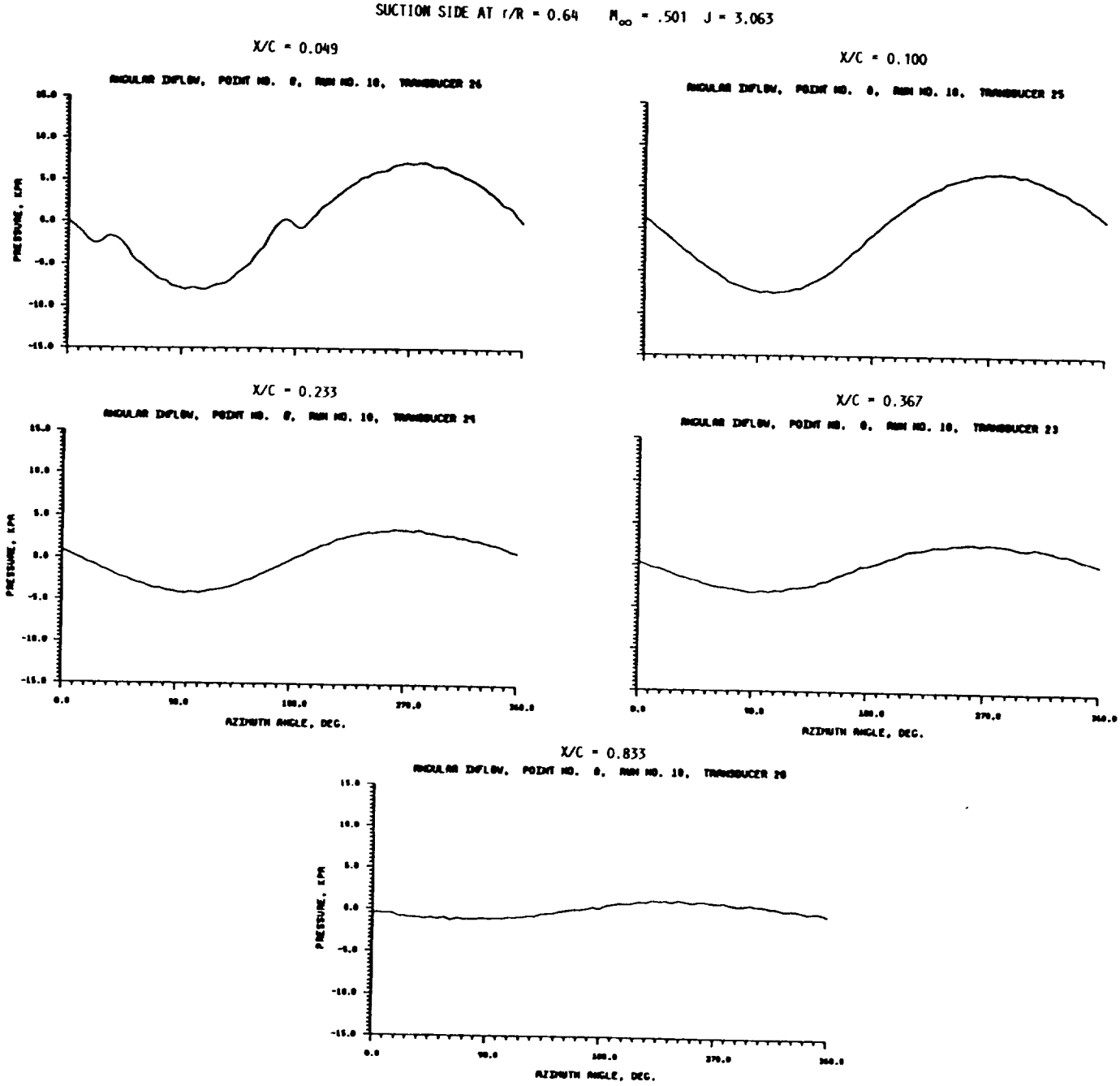

FIGURE 14. - BLADE SURFACE PRESSURE AS FUNCTION OF AZIMUTH LOCATION FOR CRUISE CONDITION WITH ANGULAR INFLOW.

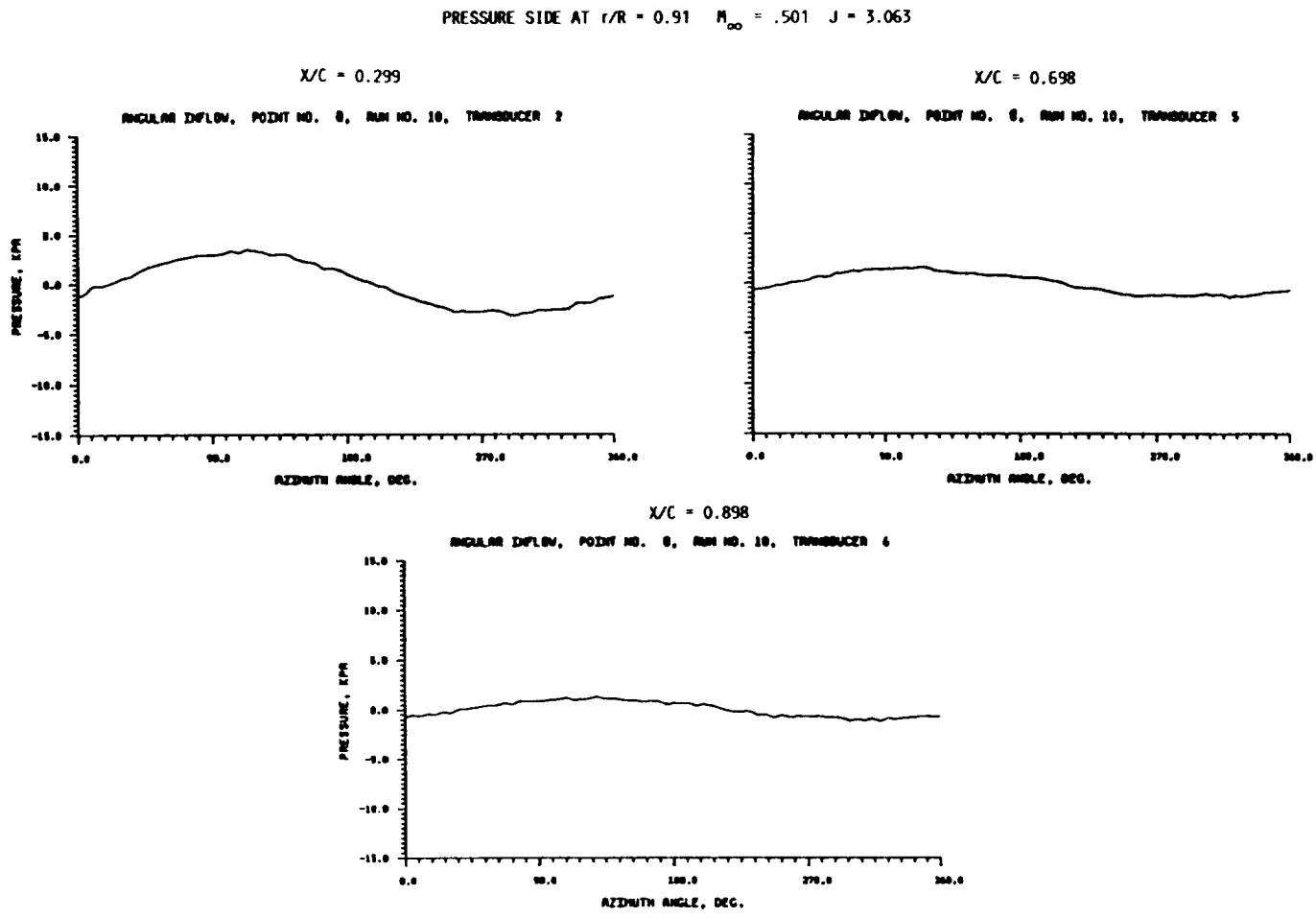

FIGURE 15. - BLADE SURFACE PRESSURE AS FUNCTION OF AZIMUTH LOCATION FOR CRUISE CONDITION WITH ANGULAR INFLOW.

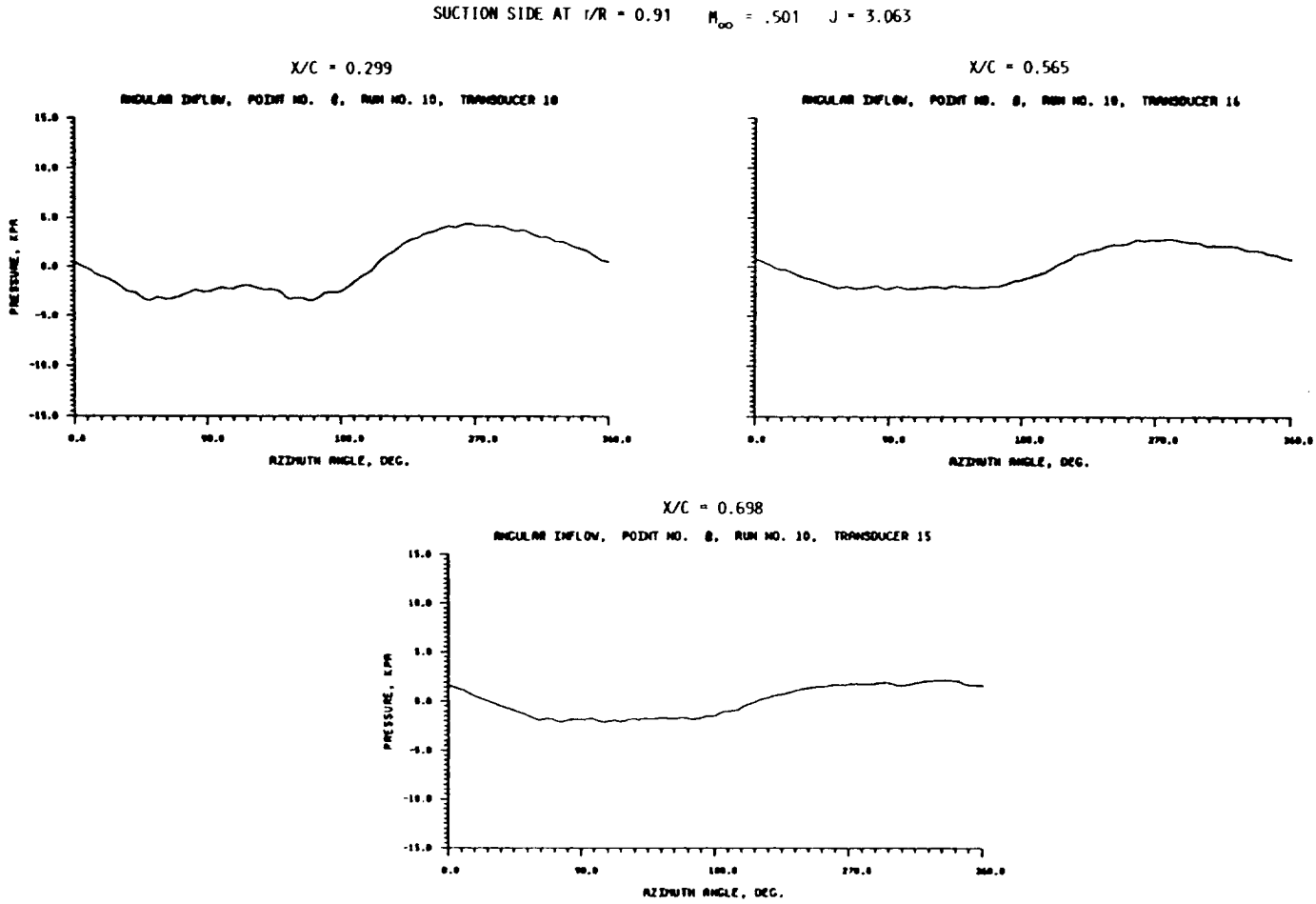

FIGURE 16. - BLADE SURFACE PRESSURE AS FUNCTION OF AZIMUTH LOCATION FOR CRUISE CONDITION WITH ANGULAR INFLOW.

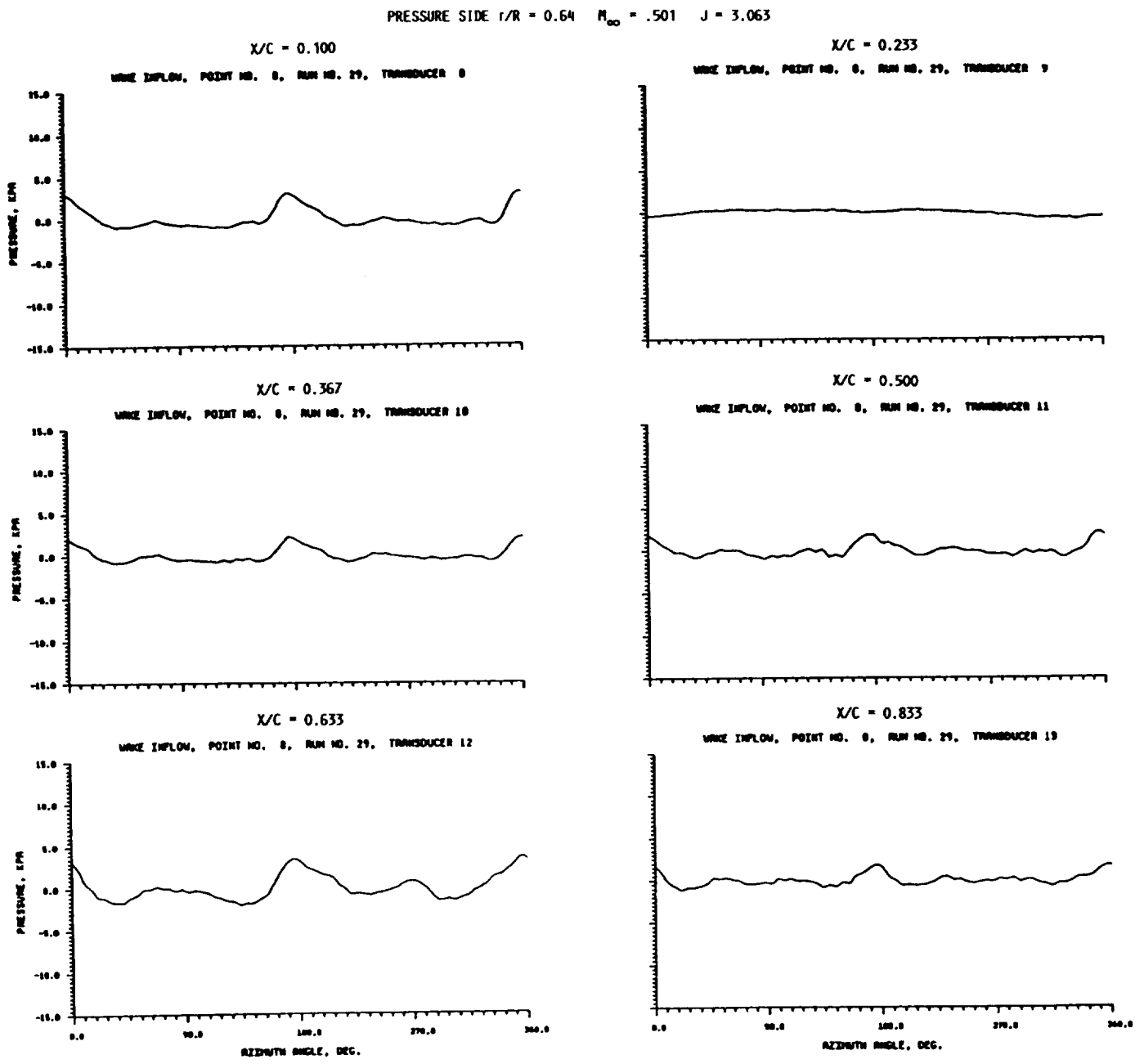

FIGURE 17. - BLADE SURFACE PRESSURE AS FUNCTION OF AZIMUTH LOCATION FOR CRUISE CONDITION WITH WAKE INFLOW.

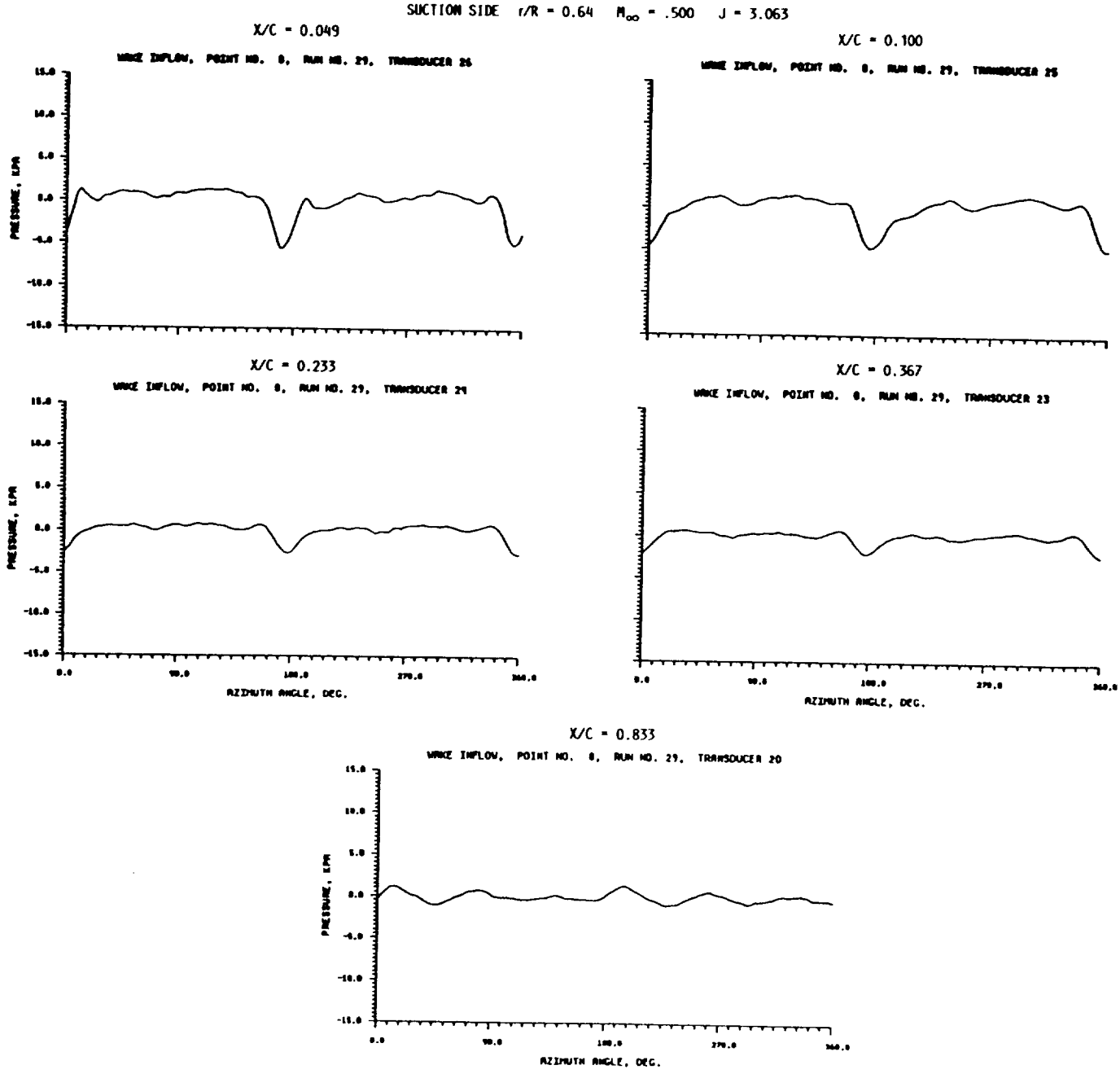

FIGURE 18. - BLADE SURFACE PRESSURE AS FUNCTION OF AZIMUTH LOCATION FOR CRUISE CONDITION WITH WAKE INFLOW.

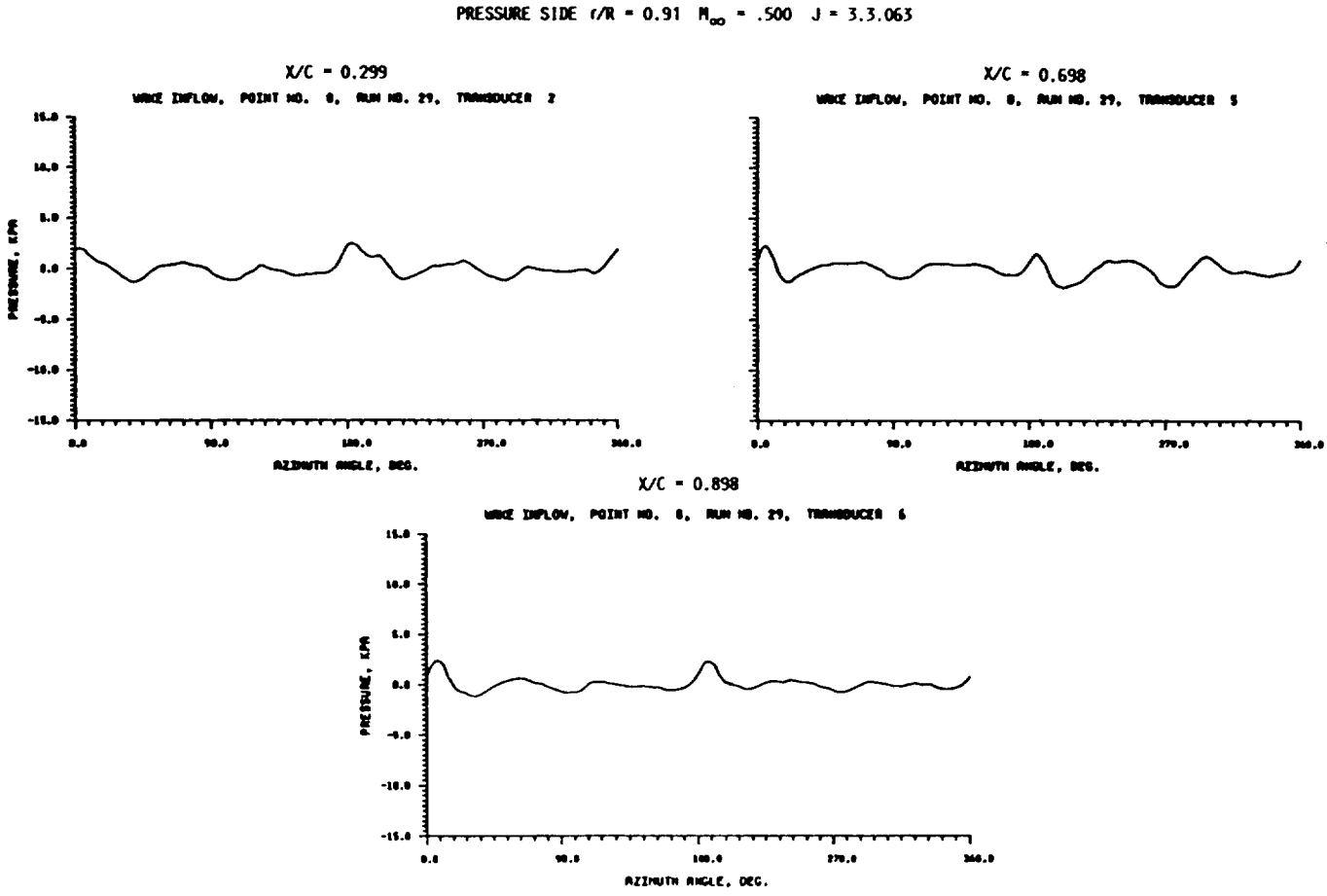

FIGURE 19. - BLADE SURFACE PRESSURE AS FUNCTION OF AZIMUTH LOCATION FOR CRUISE CONDITION WITH WAKE INFLOW.

ORIGINAL PAGE IS
OF POOR QUALITY

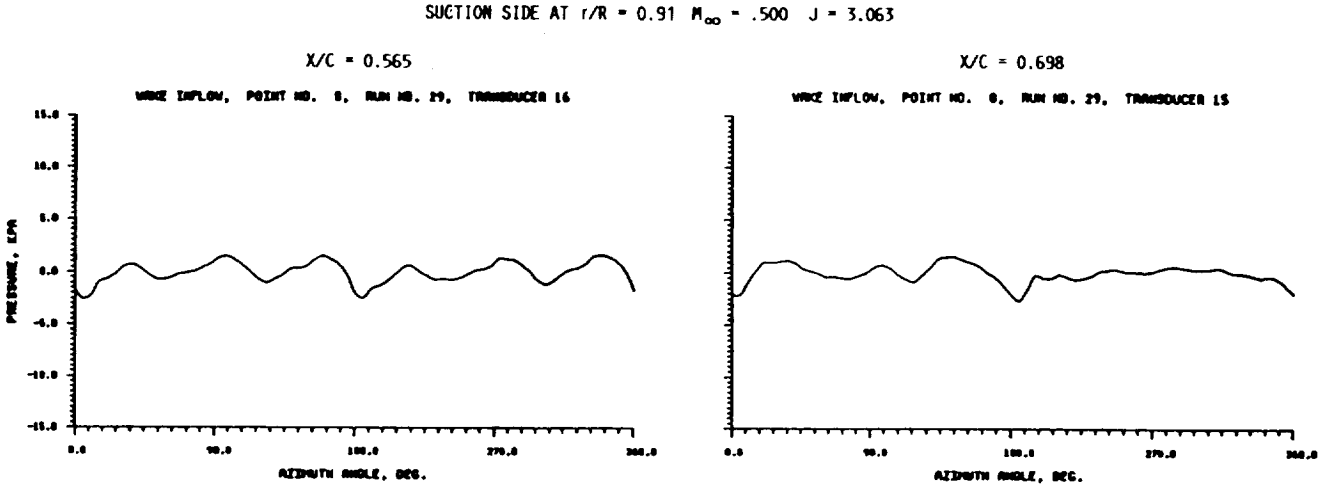

FIGURE 20. - BLADE SURFACE PRESSURE AS FUNCTION OF AZIMUTH LOCATION FOR CRUISE CONDITION WITH WAKE INFLOW.

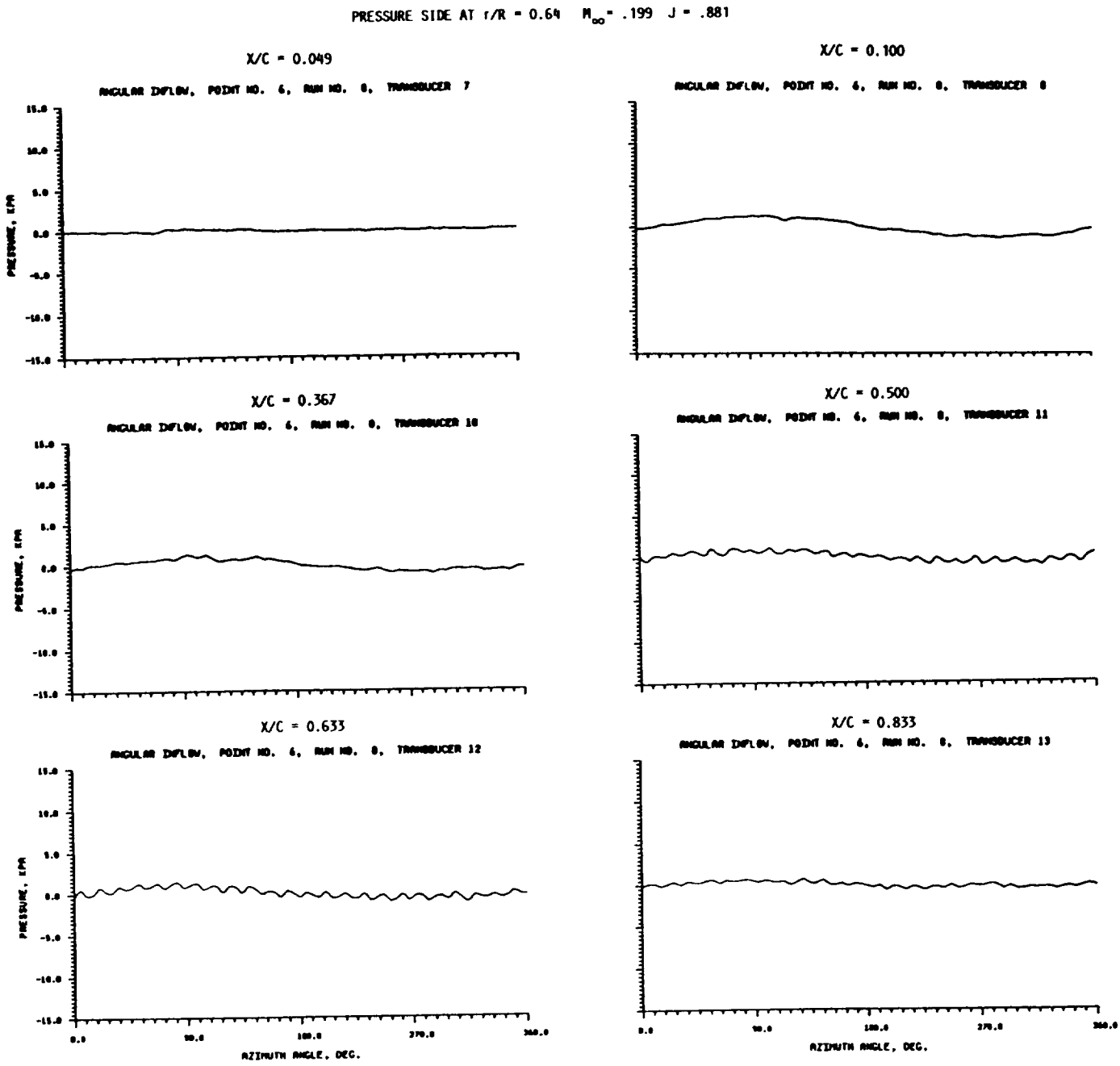

FIGURE 21. - BLADE SURFACE PRESSURE AS FUNCTION OF AZIMUTH LOCATION FOR TAKEOFF CONDITION WITH ANGULAR INFLOW.

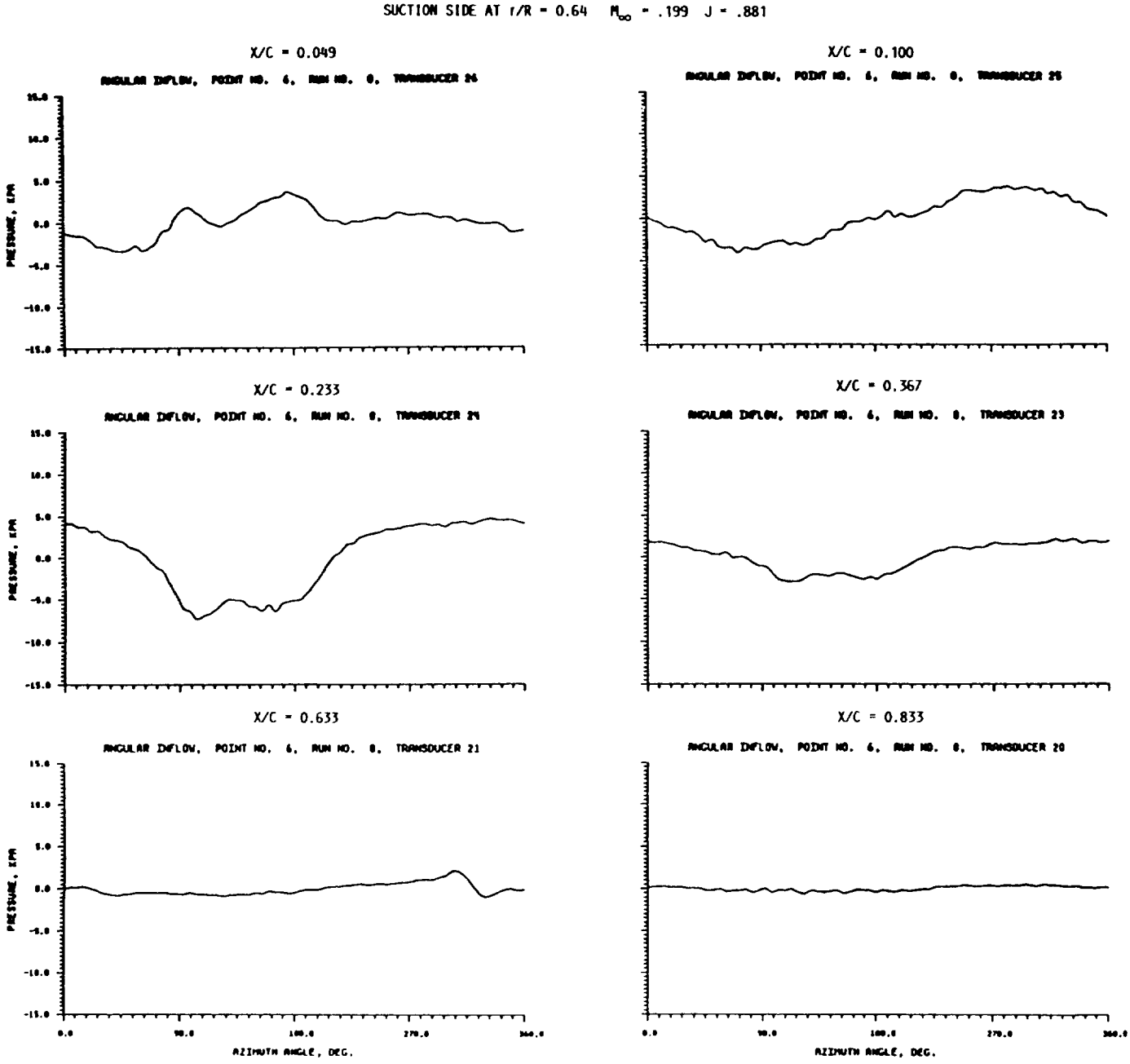

FIGURE 22. - BLADE SURFACE PRESSURE AS FUNCTION OF AZIMUTH LOCATION FOR TAKEOFF CONDITION WITH ANGULAR INFLOW.

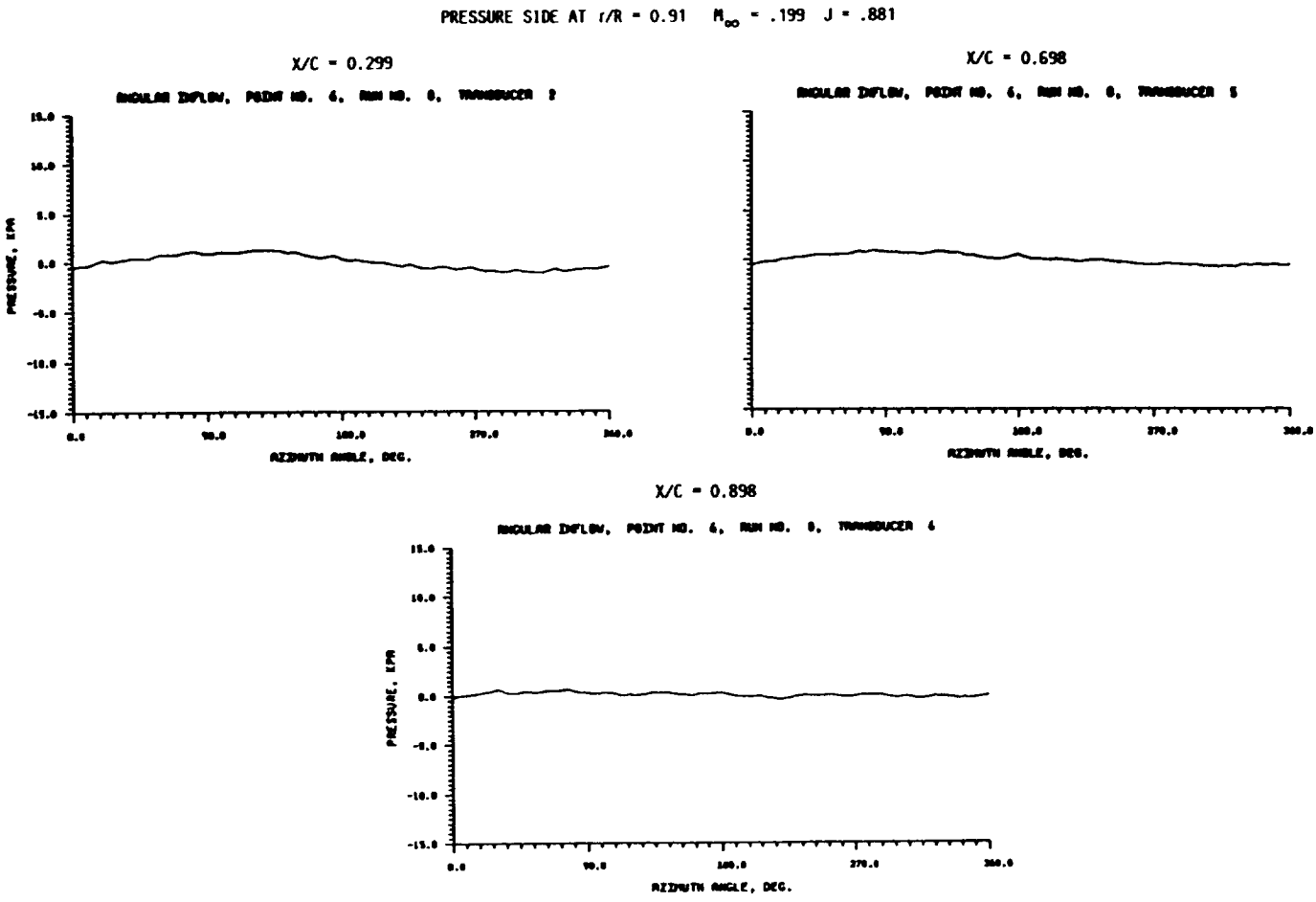

FIGURE 23. - BLADE SURFACE PRESSURE AS FUNCTION OF AZIMUTH LOCATION FOR TAKEOFF CONDITION WITH ANGULAR INFLOW.

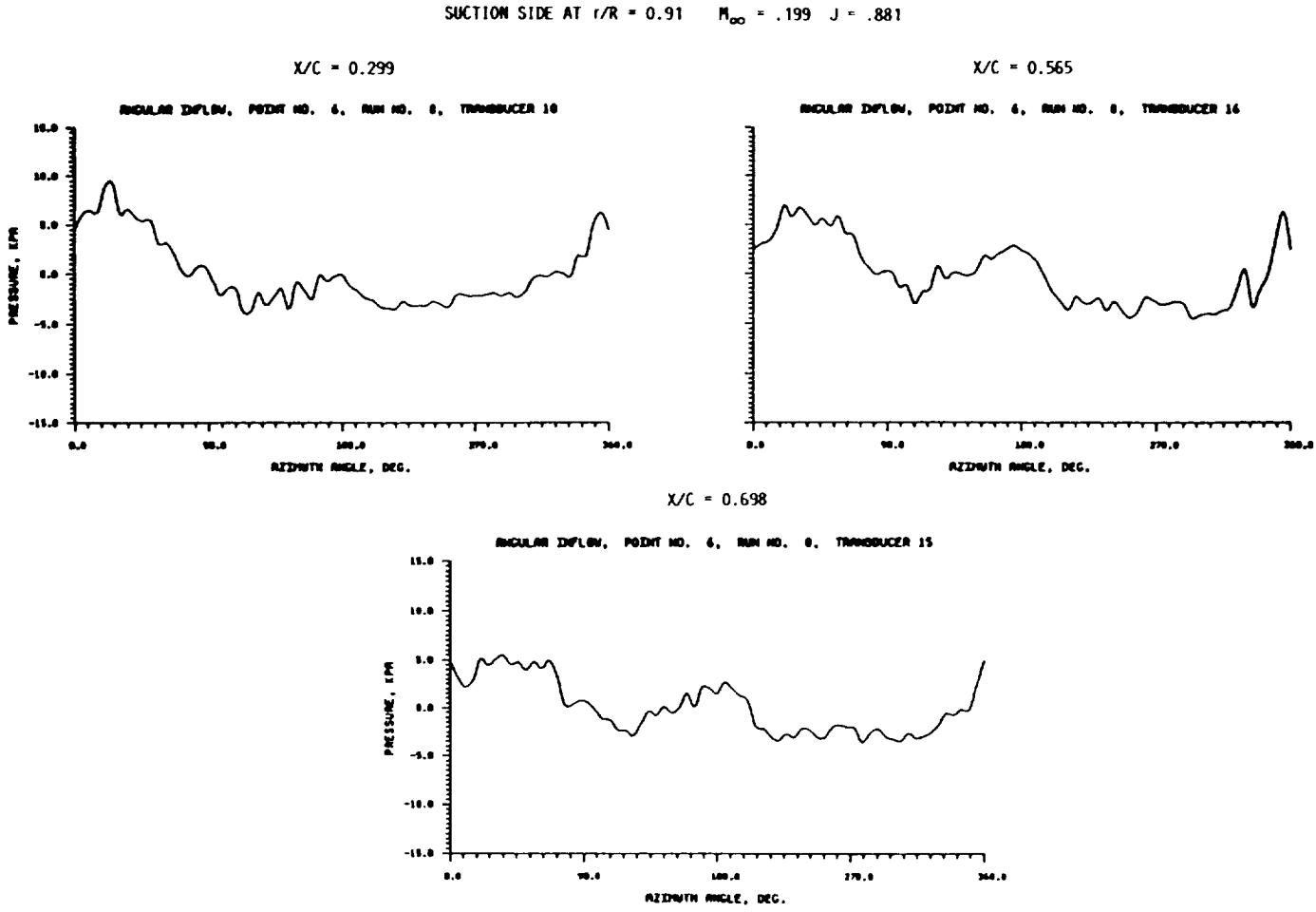

FIGURE 24. - BLADE SURFACE PRESSURE AS FUNCTION OF AXIMUTH LOCATION FOR TAKEOFF CONDITON WITH ANGULAR INFLOW.

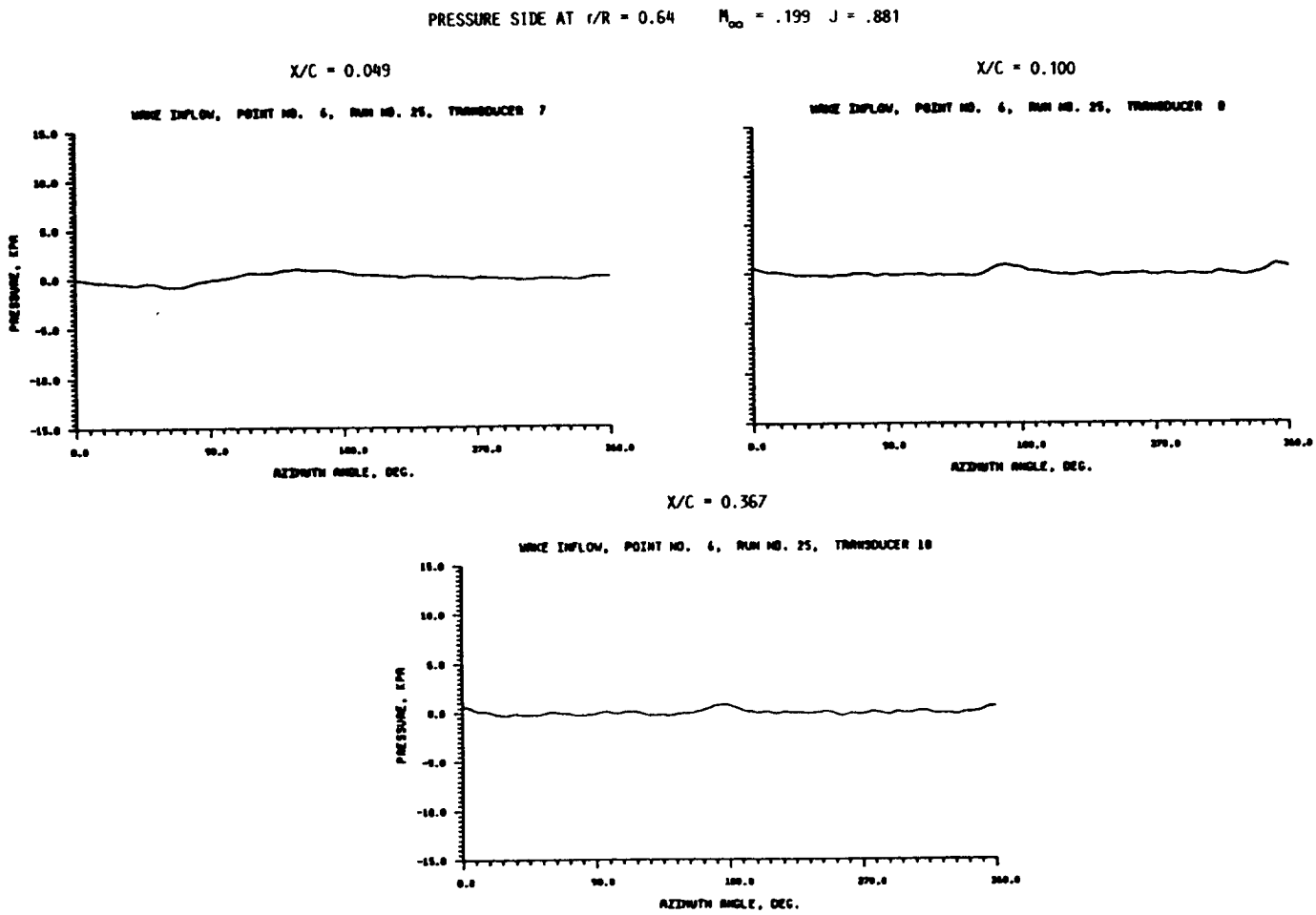

FIGURE 25. - BLADE SURFACE PRESSURE AS FUNCTION OF AXIMUTH LOCATION FOR TAKEOFF CONDITON WITH ANGULAR INFLOW.

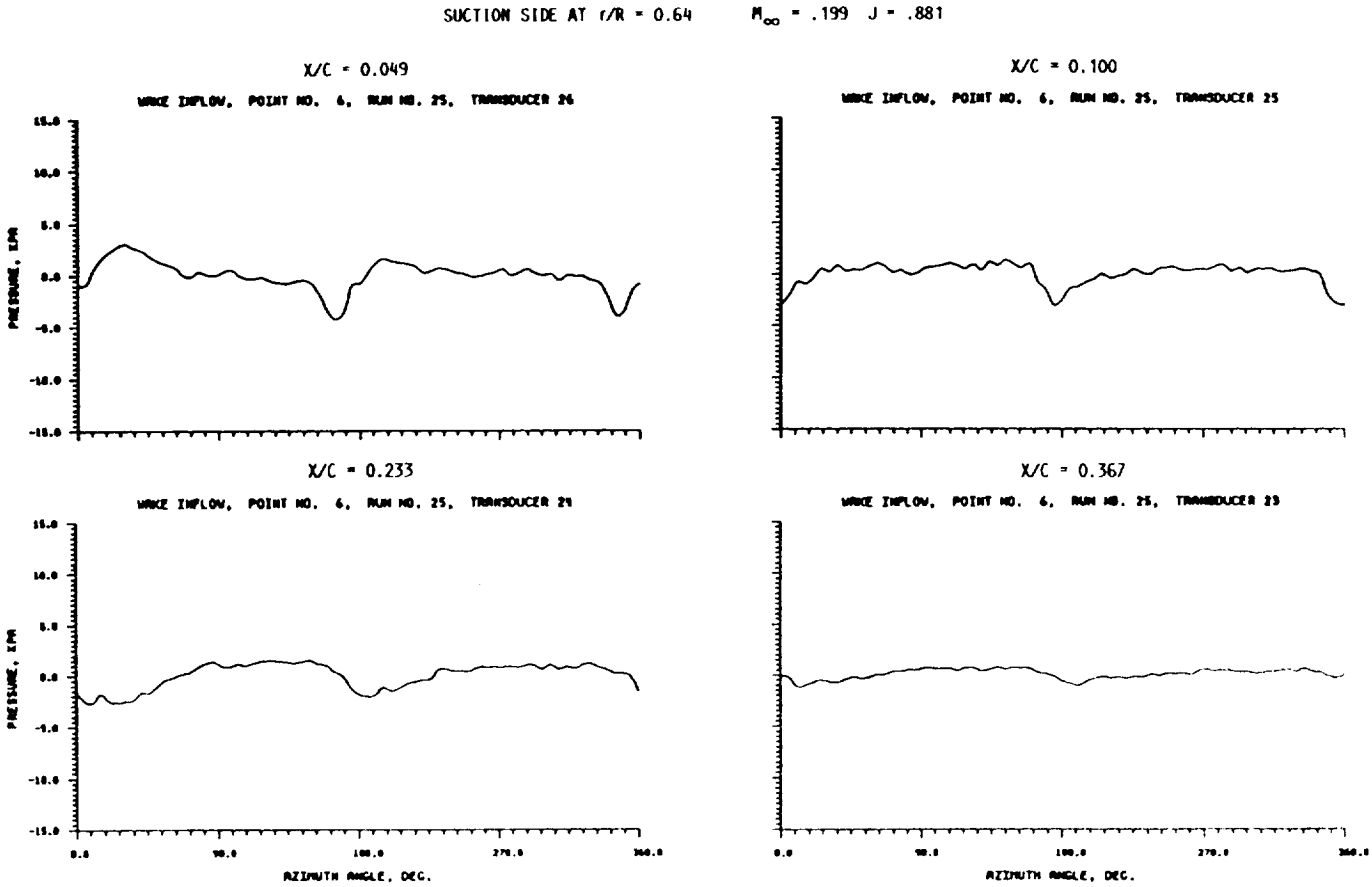

FIGURE 26. - BLADE SURFACE PRESSURE AS FUNCTION OF AXIMUTH LOCATION FOR TAKEOFF CONDITION WITH WAKE INFLOW.

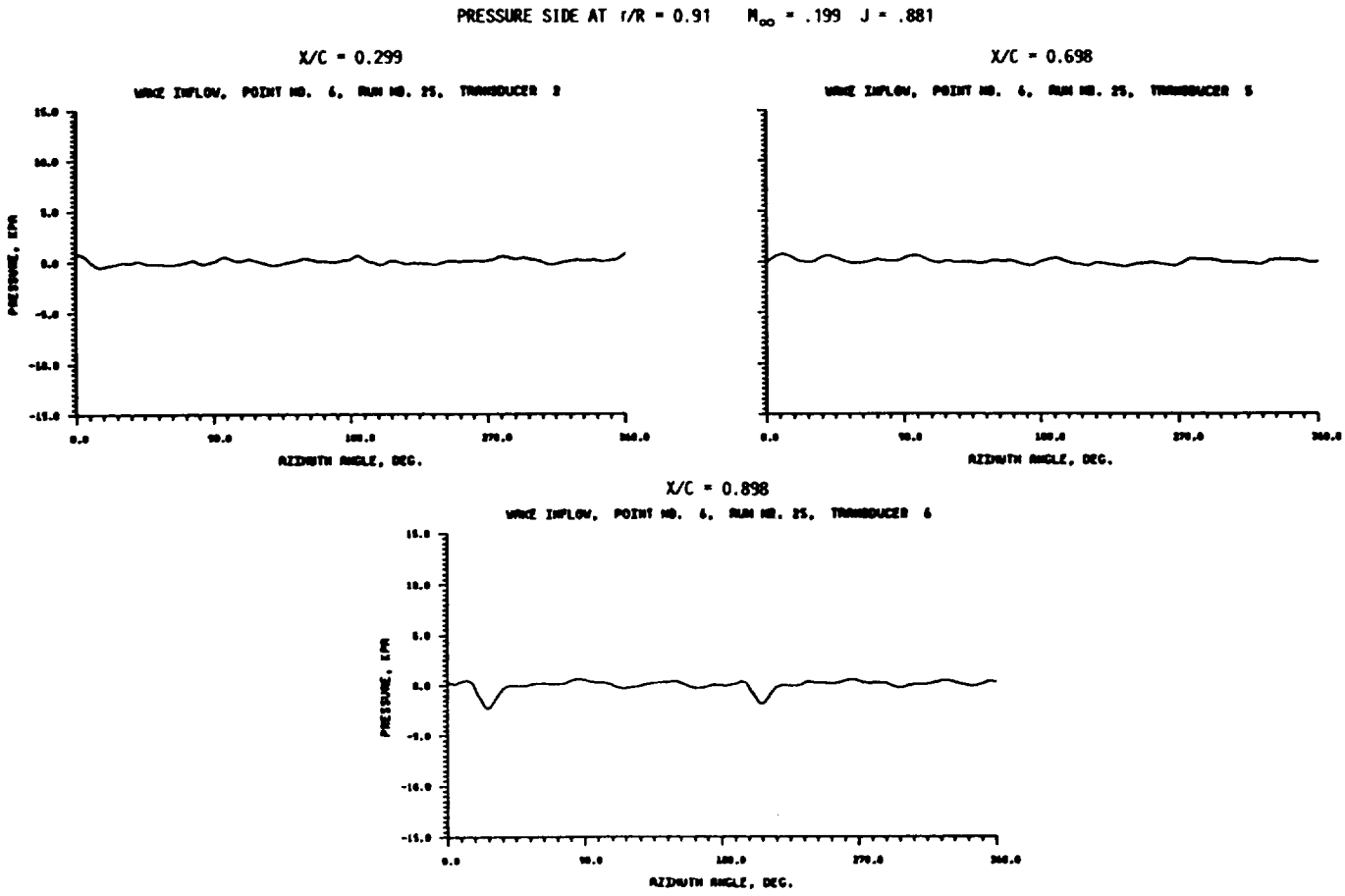

FIGURE 27. - BLADE SURFACE PRESSURE AS FUNCTION OF AZIMUTH LOCATION FOR TAKEOFF CONDTION WITH WAKE INFLOW.

SUCTION SIDE AT r/R = 0.91 M_{∞} = .199 J = .188

X/C = 0.565

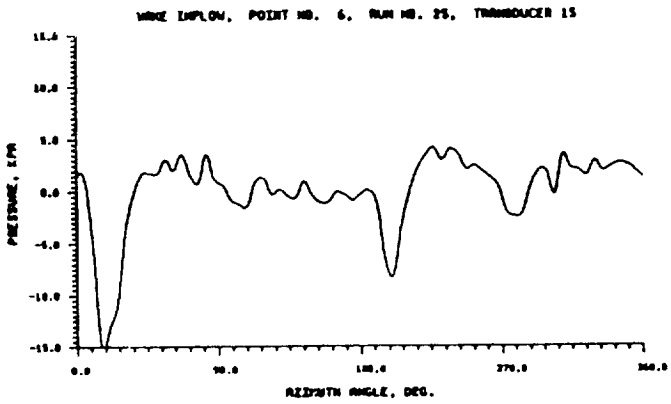

X/C = 0.698

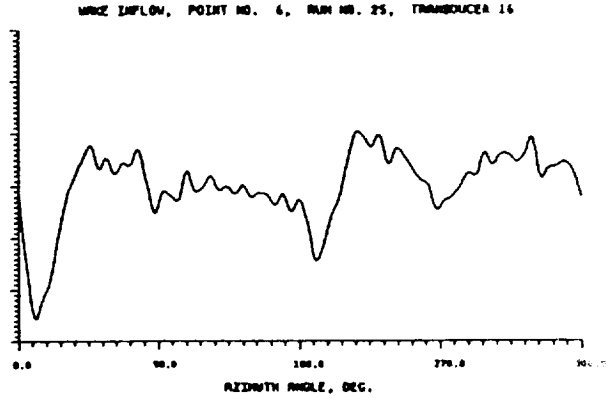

FIGURE 28. - BLADE SURFACE PRESSURE AS FUNCTION OF AZIMUTH LOCATION FOR TAKEOFF CONDITION WITH WAKE INFLOW.

NASA
National Aeronautics and Space Administration

Report Documentation Page

1. Report No.	2. Government Accession No.	3. Recipient's Catalog No.
NASA CR-182123		

4. Title and Subtitle

Measurement of Unsteady Blade Surface Pressure on a Single Rotation Large Scale Advanced Prop-Fan With Angular and Wake Inflow at Mach Numbers From 0.02 to 0.70

5. Report Date

October 1988

6. Performing Organization Code

7. Author(s)

P. Bushnell, M. Gruber, and D. Parzych

8. Performing Organization Report No.

None (E-4137)

10. Work Unit No.

505-03-01

9. Performing Organization Name and Address

Hamilton Standard Division
United Technologies Corporation
Windsor Locks, Connecticut 06096

11. Contract or Grant No.

NAS3-23051

13. Type of Report and Period Covered

Contractor Report
Final

12. Sponsoring Agency Name and Address

National Aeronautics and Space Administration
Washington, D.C. 20546-0001

14. Sponsoring Agency Code

15. Supplementary Notes

Project Manager, Julius J. Notardonato, Propulsion Systems Division, NASA Lewis Research Center. The microfiche supplement at the back of the report contains the appendixes listed in the Contents.

16. Abstract

Unsteady aerodynamic pressures were measured on the surface of a rotating Prop-Fan blade in an experiment performed by Hamilton Standard Division of United Technologies Corporation, under contract to NASA-Lewis Research Center, at the S1-MA wind tunnel facility operated by the office National D'Etudes et de Recherches Aerospatiale (ONERA) in Modane, France. The objectives of the experiment were to measure the periodic variations of blade surface pressure resulting from two non-uniform inflow conditions: first, inflow at a three degree angle to the Prop-Fan axis of rotation, and second, inflow with a wake generated by a cylinder mounted upstream of the rotor. In addition, unsteady pressures were measured under uniform inflow conditions to determine background response levels. The range of Prop-Fan operating conditions included inflow Mach numbers from 0.02 to 0.70. For most of the inflow Mach numbers, more than one power coefficient and/or advance ratio was investigated. Due to facility power limitations the Prop-Fan test installation was a two bladed version of the eight bladed design configuration. The power coefficient range investigated was therefore selected to cover typical power loading per blade conditions which occur within the Prop-Fan operating envelope. This report provides unsteady blade surface pressure data for the LAP Prop-Fan blade operation with angular inflow, wake inflow and uniform flow over a range of inflow Mach numbers of 0.02 to 0.70. The data are presented as Fourier coefficients for the first 35 harmonics of shaft rotational frequency. Also presented is a brief discussion of the unsteady blade response observed at takeoff and cruise conditions with angular and wake inflow.

17. Key Words (Suggested by Author(s))	18. Distribution Statement
Prop-Fan	Date for general release October 1990. Subject Category 07

19. Security Classif. (of this report)	20. Security Classif. (of this page)	21. No of pages	22. Price*
Unclassified	Unclassified	45	A03